Introduction

We now turn to older neutron stars in low mass X-ray binaries (LMXBs).

These systems have lower B-fields

$\Longrightarrow$ no pulsations observed

What we will talk about:

- Spectral Shape/ Classification

  Atoll-sources, Z-sources, Dippers

- X-ray Bursts
- Rapid Time Variability
- Accretion Disk Corona Sources

Table 1 Bright low-mass X-ray binaries[a]

Source name(s)	l^{II}, b^{II} (°)	I_x[b] Mean (μJy)	Min. (μJy)	Max. (μJy)	P_{orb}[c] (hr)	Type[d]	Phenomenology[e]
Sco X-1 (1617−155)	359+24	12,400	9300	16,300	19.2	Z	QPO
GX 5−1 (1758−250)	5−1	1200	1070	1410	—	Z	QPO
GX 349+2 (1702−363)[f]	349+3	780	620	980	—	Z	QPO
GX 17+2 (1813−140)	16+1	680	600	780	19.8?[g]	Z	QPO, (bu)
GX 9+1 (1758−205)	9+1	650	550	720	—	A	—
GX 340+0 (1642−455)	340−0	490	400	620	—	Z	QPO
GX 3+1 (1744−265)	2+1	430	230	550	—	A	QPO, (Bu)
Cyg X-2 (2142+380)	87−11	430	290	730	235	Z	QPO, (bu), Mo
GX 13+1 (1811−171)	14+0	340	240	430	—	A	—
GX 9+9 (1728−169)	8+9	290	230	340	4.2	A	Mo
4U 1820−30 (NGC 6624)	3−8	260	94	360	0.2	A	QPO, (Bu), Mo
4U 1705−44	343−2	260	39	440	—	A	Bu
4U 1636−53	333−5	220	100	320	3.8	A	Bu
Ser X-1 (1837+049)	36+5	200	150	290	—	—	Bu
GCX-1 (1742−294)	0−0	170	130	270	—	—	Bu?
4U 1728−33	354−0	170	140	190	—	A	Bu
GX 339−4 (1659−487)	339−4	160	36	250	14.8?	—	QPO, BH?[h]
4U 1735−44	346−7	160	110	210	4.6	A	Bu

[a] All variable objects in 3A Catalogue (69, 153) with an average flux ≥100 μJy not identified with an early-type star (excluding Cyg X-3).

[b] Converted from *Ariel V* ASM counts into μJy (2–11 keV) according to 1 ASM c/s = 2.6 μJy (9).

[c] See (84).

[d] Z or A(toll) source; see text. After (36).

[e] QPO: all reported quasi-periodic oscillations are indicated here (see Section 3 for an evaluation of QPO reports in atoll sources); Bu: regular X-ray bursts; (Bu): has shown an episode of regular X-ray bursts; (bu): occasional X-ray bursts reported; BH?: black hole candidate, Mo: shows periodic X-ray modulation (9, 55, 64).

[f] "Sco X-2."

[g] Reference: (37).

[h] References: (77, 157).

(van der Klis, 1989, Tab. 1)

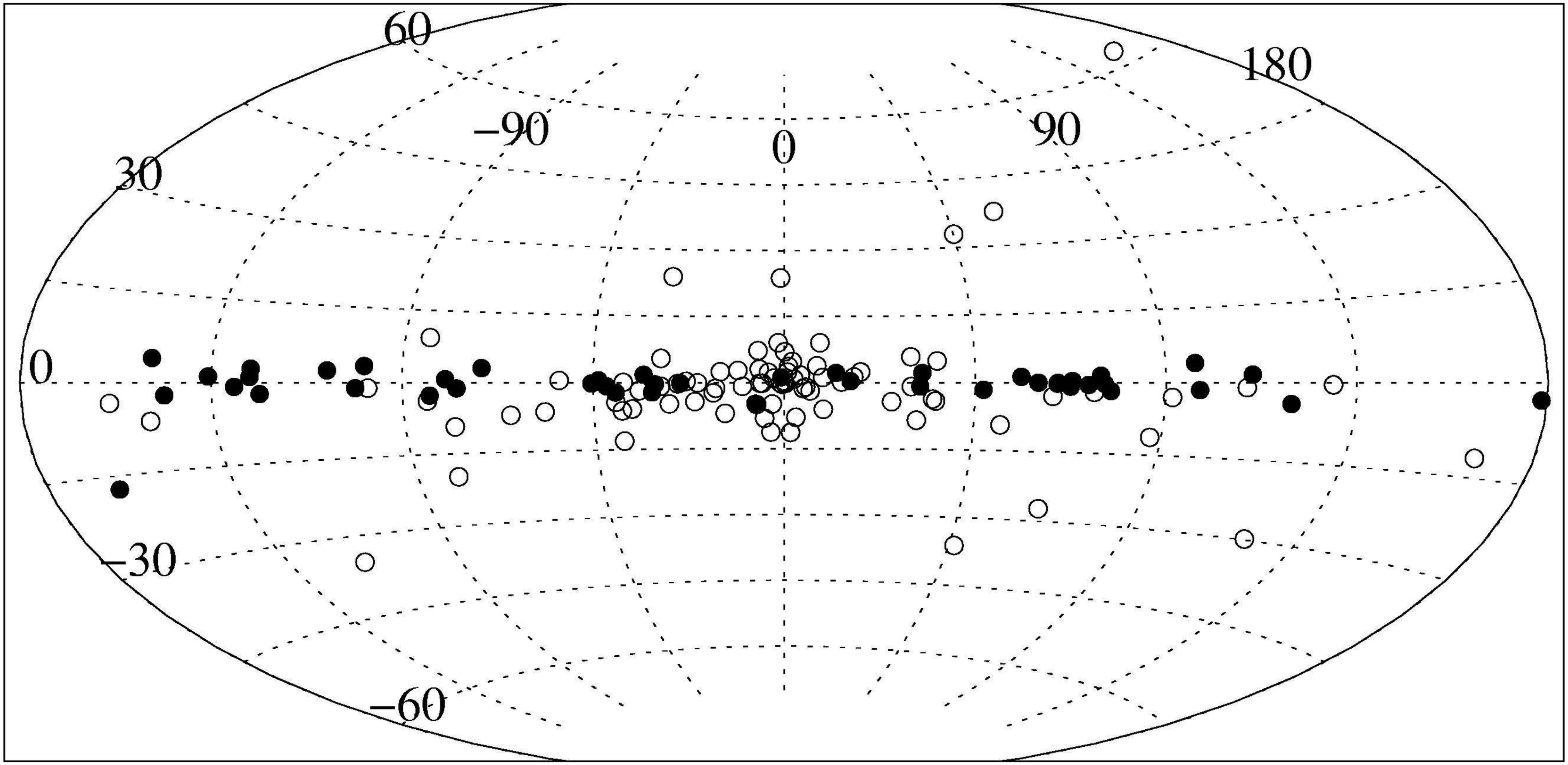

(Grimm, Gilfanov & Sunyaev, 2003)

Distribution of HMXB (filled circles) and LMXB (open circles) in the Galaxy

Classifi cation

Hasinger & van der Klis (1989): "Two patterns of correlated X-ray timing and spectral behaviour in low-mass X-ray binaries"

Source classification through their behavior in the color-color-diagram or in the Hardness-Intensity-Diagram:

Here, we define an X-ray color (or "hardness ratio"):

$$\text{color} = \frac{\text{CR}_{\text{upper energy band}}}{\text{CR}_{\text{lower energy band}}} \tag{6.1}$$

where CR_i is the measured count rate in a given energy band.

Typical bands used depend on the satellite, typical width is a few keV!

Z-sources, I

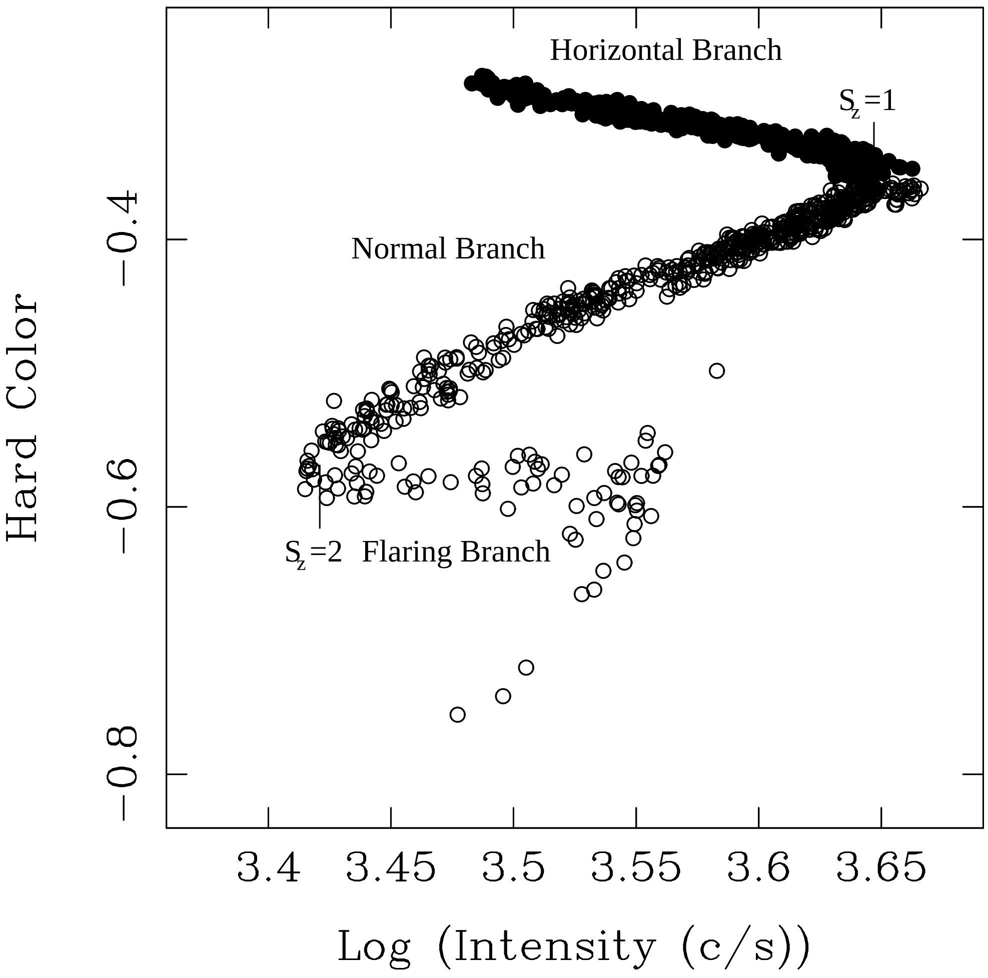

(GX 340+0; Jonker et al., 2000)

Z-sources: higher luminosity LMXBs (L_X close to L_{Edd}).

Color-intensity-diagram:

- horizontal branch: characterized by 20–50 Hz "Horizontal Branch Oscillations" (HBOs) and strong variability (including quasi-periodic oscillations, QPOs)
- normal branch: much weaker variability

  pre 1988 people thought this behavior to be the normal one for neutron star LMXB.
- flaring branch: spectrum mostly thermal

  Named after flares in Sco X-1

Intensity described with S_Z-parameter along the Z.

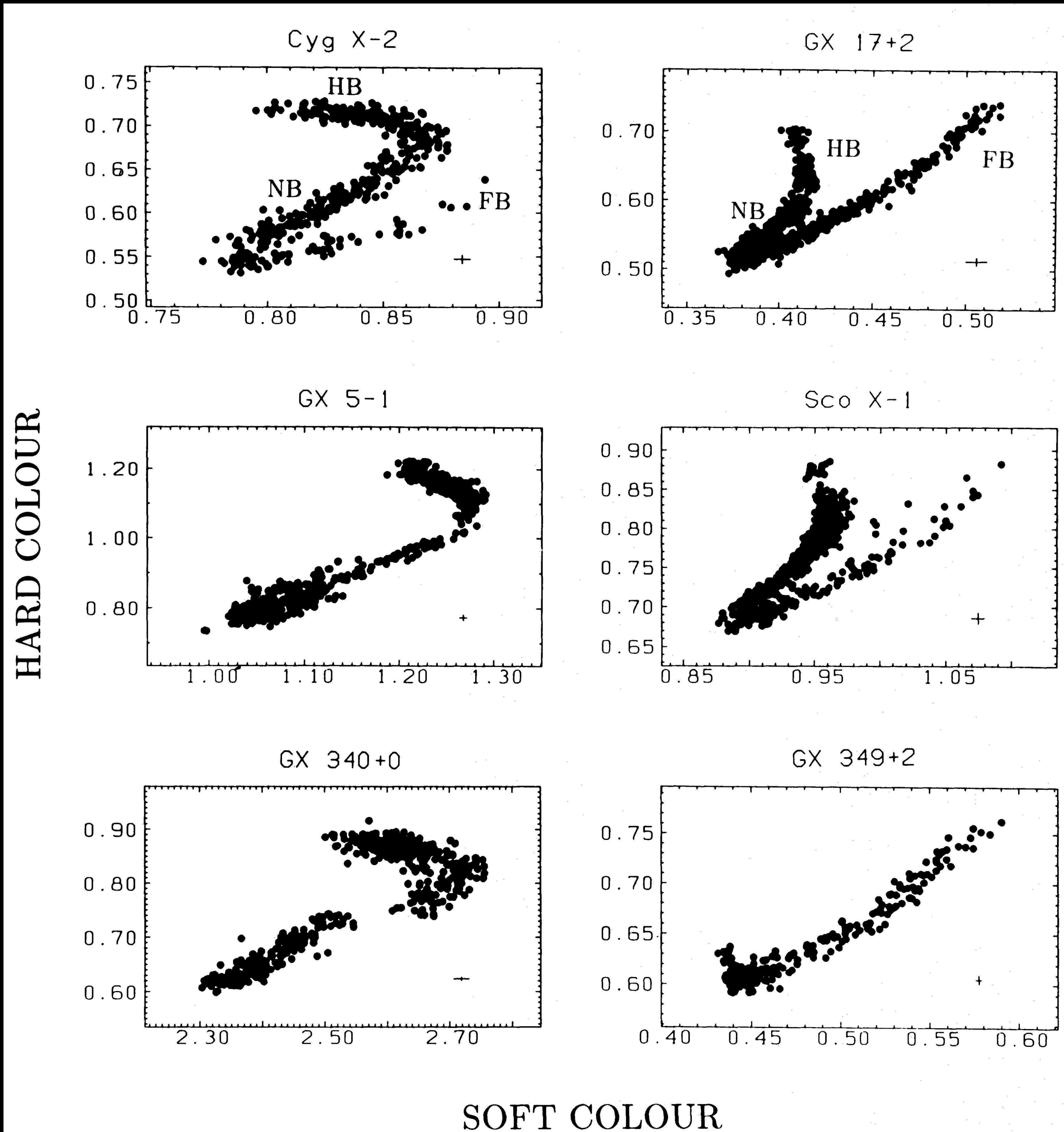

Depending on the source and choice of color bands, the Z is can be rather severely distorted.

(Hasinger & van der Klis, 1989, Fig. 1a)

Atoll sources

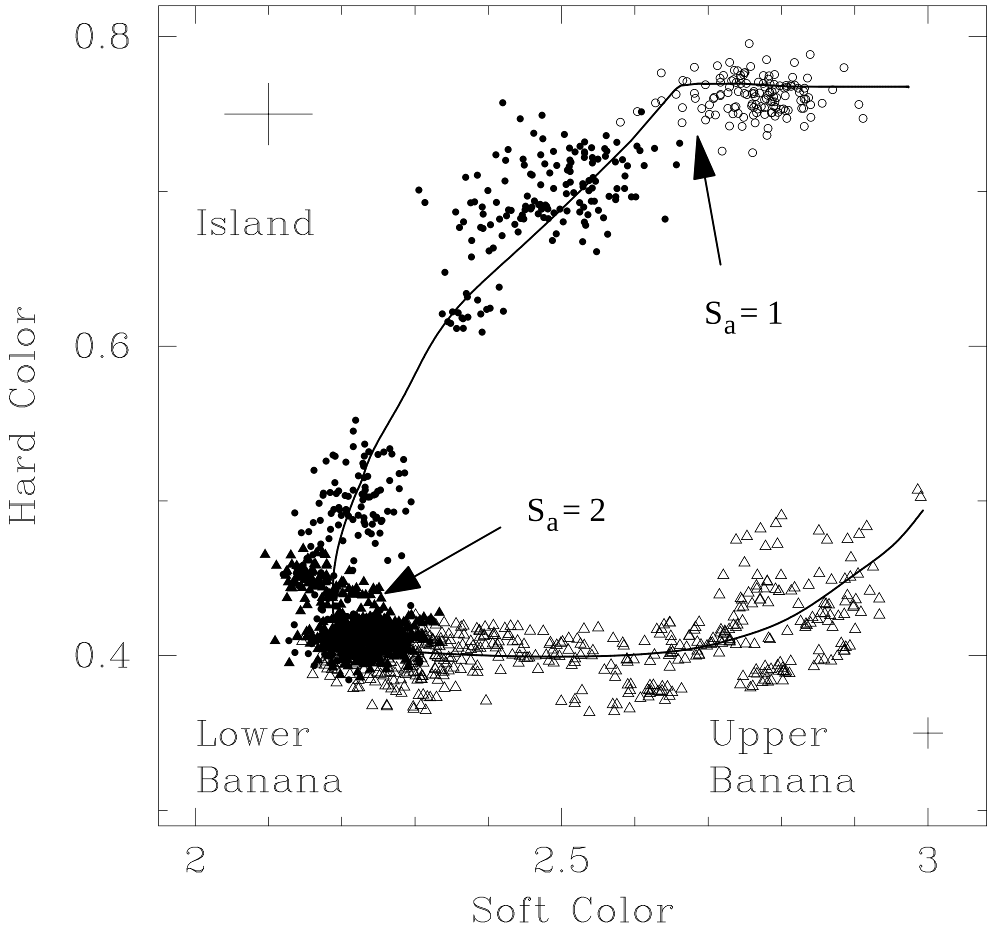

(4U1608−52; Méndez et al., 1999)

Atoll sources: generally lower luminosity than Z-sources; color-color-diagram looks like a pacific island

Intensity increases with parameter S_a:

- banana state: higher luminosity state, variability dominated by low frequency noise
- island state: lower luminosity state, variability dominated by high frequency noise

S_a is defined "by eye", see diagram

Typical luminosities 0.01–0.2 L_{Edd}, although four sources might be brighter than that (van der Klis, 2000)

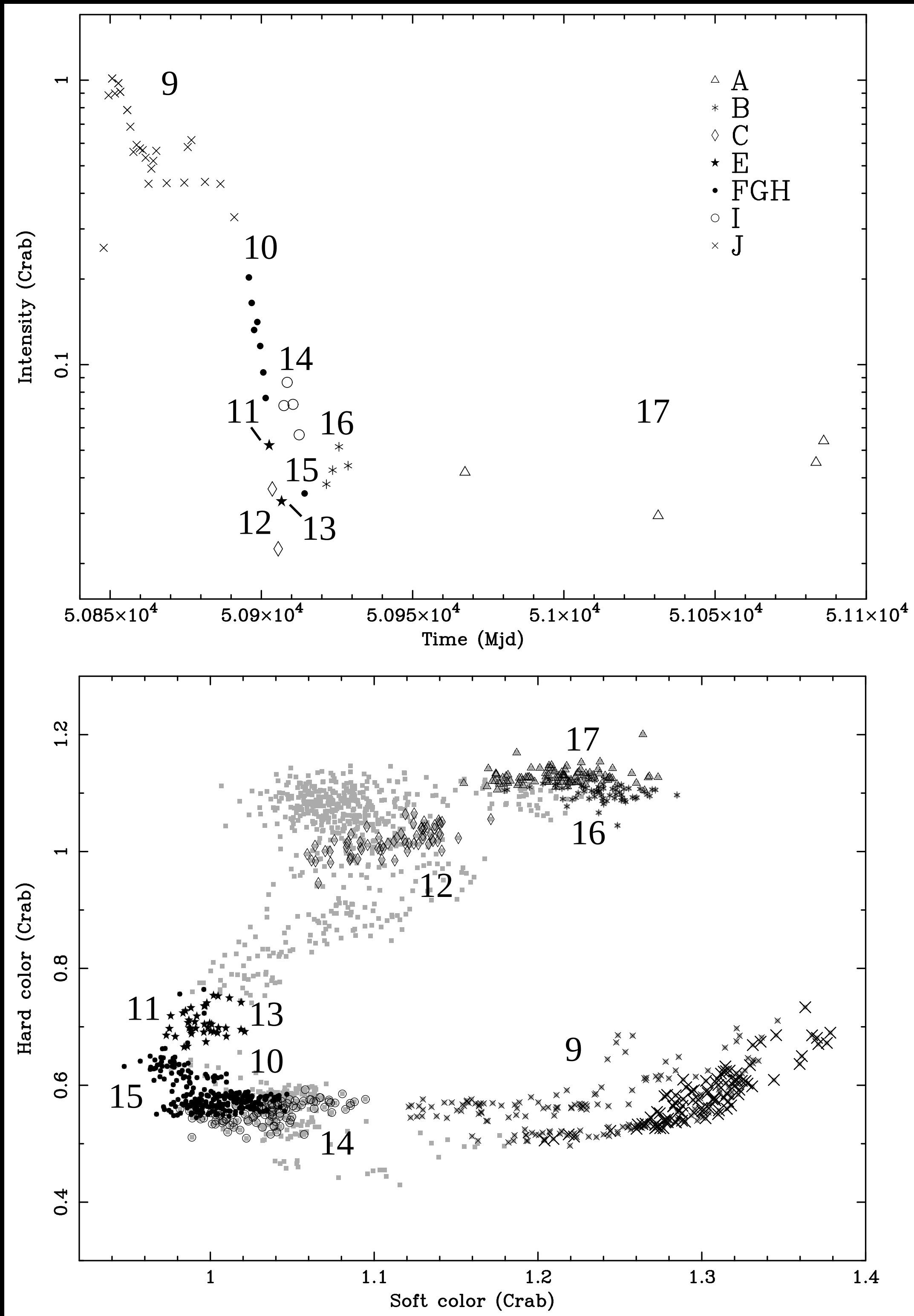

The source location in the color-color diagram varies on timescales of days to weeks

generally slower in island, faster in banana

(van Straaten, van der Klis & Méndez, 2003, Fig. 2)

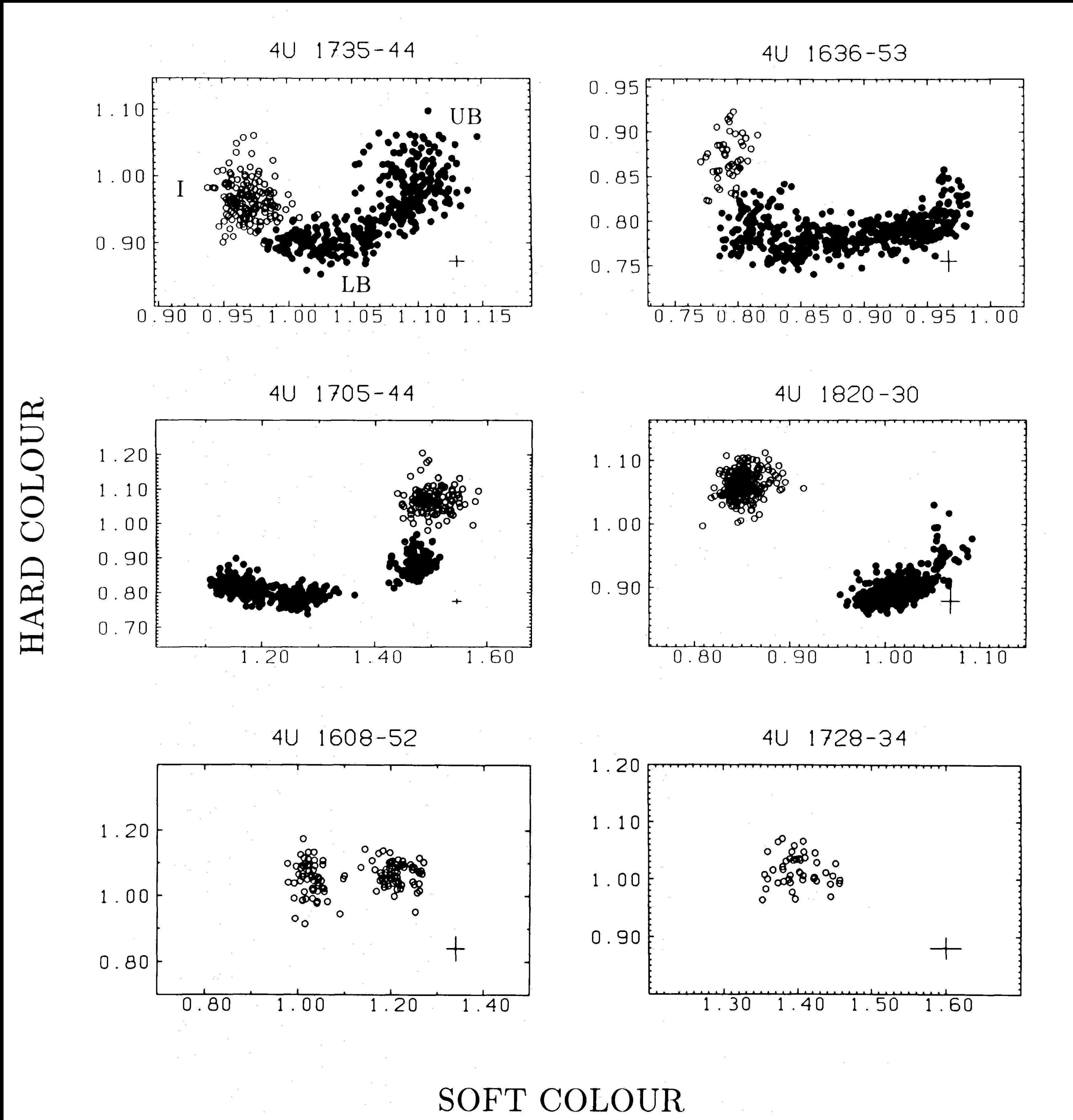

Not all sources are present in the banana and island states, depends on individual source luminosity variations.

(Hasinger & van der Klis, 1989, Fig. 3a)

Spectral shape

(White, Stella & Parmar, 1988): The spectral shape is well described by a power law with exponential cutoff,

$$N_{\mathrm{ph}}(E) \propto E^{-\Gamma} \exp\left(-\frac{E}{E_{\mathrm{fold}}}\right) \quad (6.2)$$

where

- N_{ph}: photon flux (ph cm^{-2} s^{-1} keV^{-1}),
- $\Gamma \sim$ 0–2: photon index,
- $E_{\mathrm{fold}} \sim$ 1–20 keV: folding energy (also often called cutoff energy)

Such a spectral shape probably due to Comptonization

High luminosity sources (=Z-sources) show additional black body component with $kT_{\mathrm{BB}} \sim$ 1–2 keV, contributing 10–70% of the total flux (higher L_{X} implies more BB-flux).

Often, an additional Fe Kα line at 6.4 keV is required.

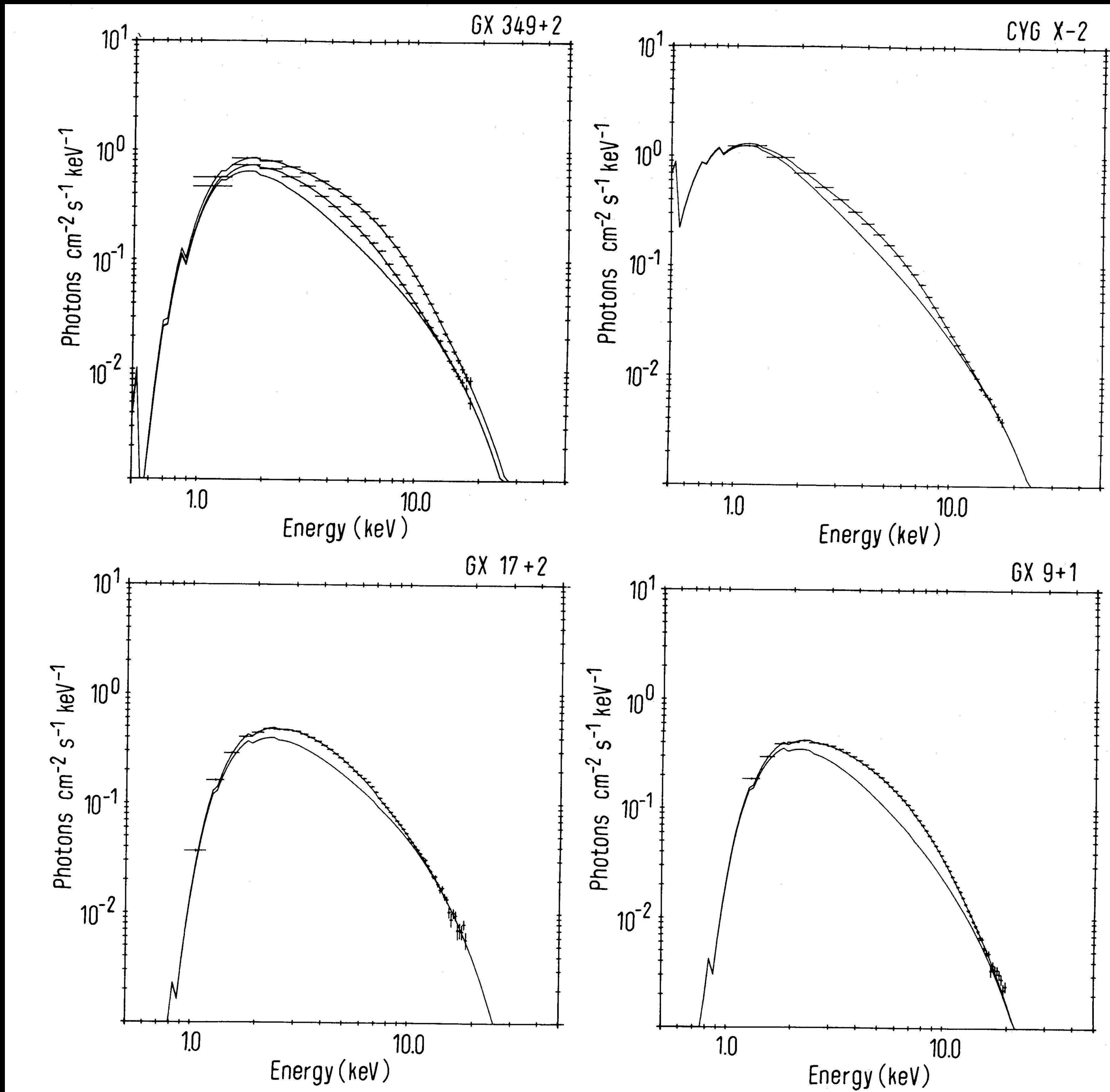

Example spectra of LMXB (White, Stella & Parmar, 1988, lower line is Comptonization only)

Spectral shape

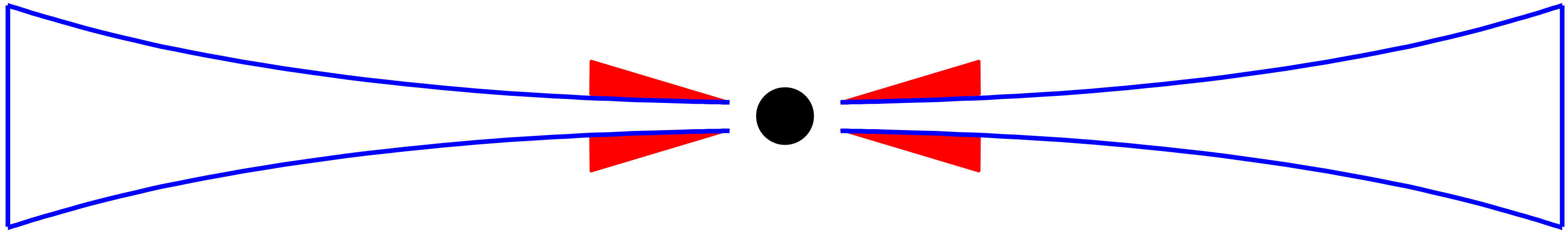

(after Church, 2004)

The interpretation of spectral shape is heavily debated.

Western model (White, Stella & Parmar, 1988) and Birmingham model (Church & Balucinska-Church, 1995):

- black body is from neutron star,
- Comptonization happens in inner edge of the accretion disk (e.g., in hot accretion disk wind).

Spectral shape

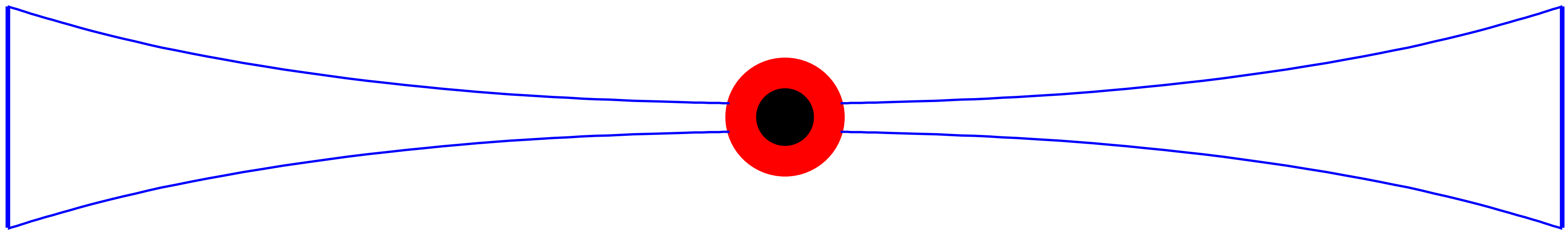

(after Church, 2004)

The interpretation of the spectral shape is heavily debated.

Eastern model (Mitsuda et al., 1989):

- Soft spectrum: thermal radiation from accretion disk

  (assuming $T(r) \propto r^{-3/4}$)

- Hard spectrum is Comptonization in neutron star atmosphere (which provides seed photons as thermal radiation).

X-Ray Bursts

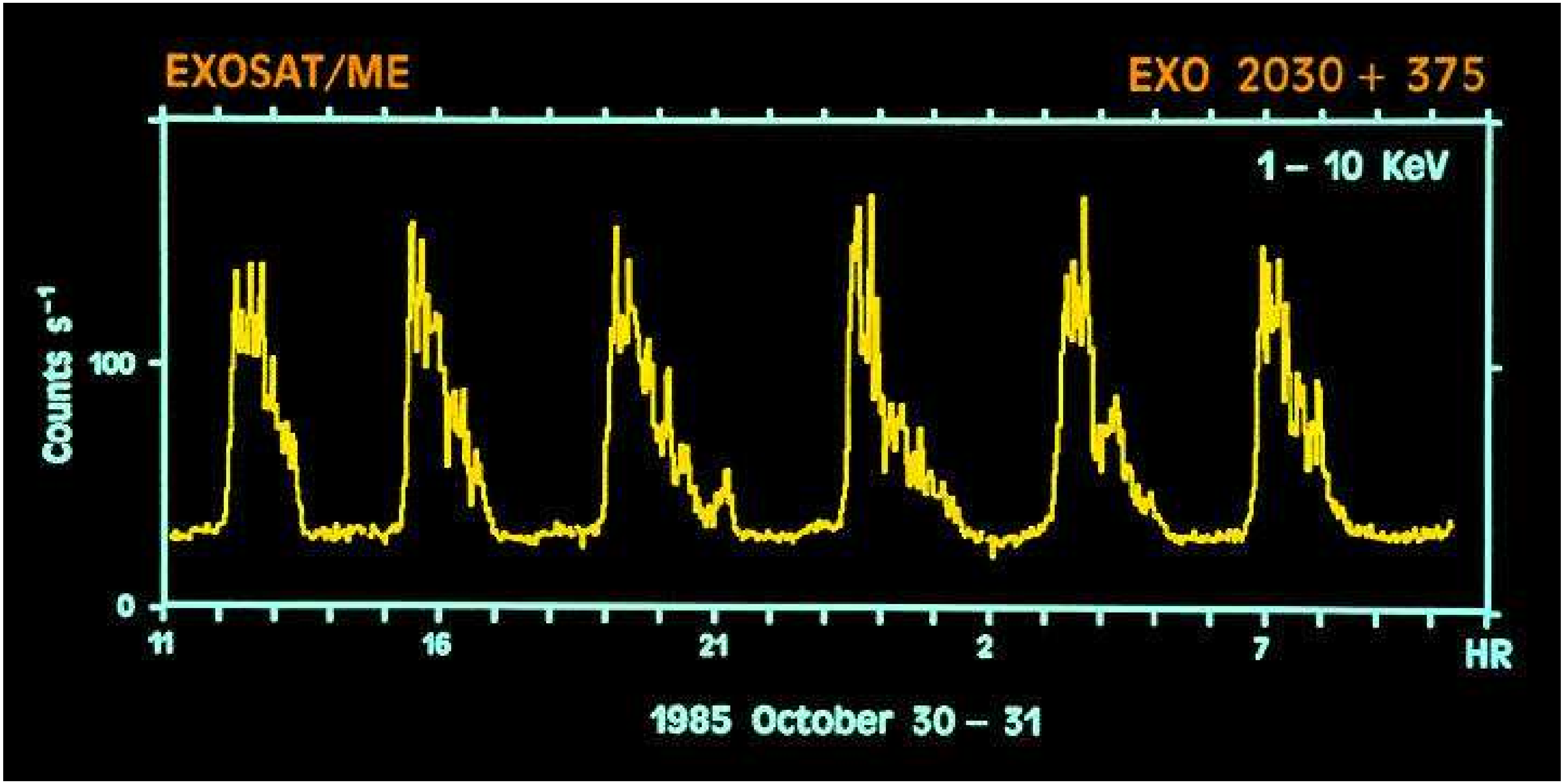

NASA GSFC

X-ray bursts from EXO 2030+375 as seen with EXOSAT.

X-Ray Bursts

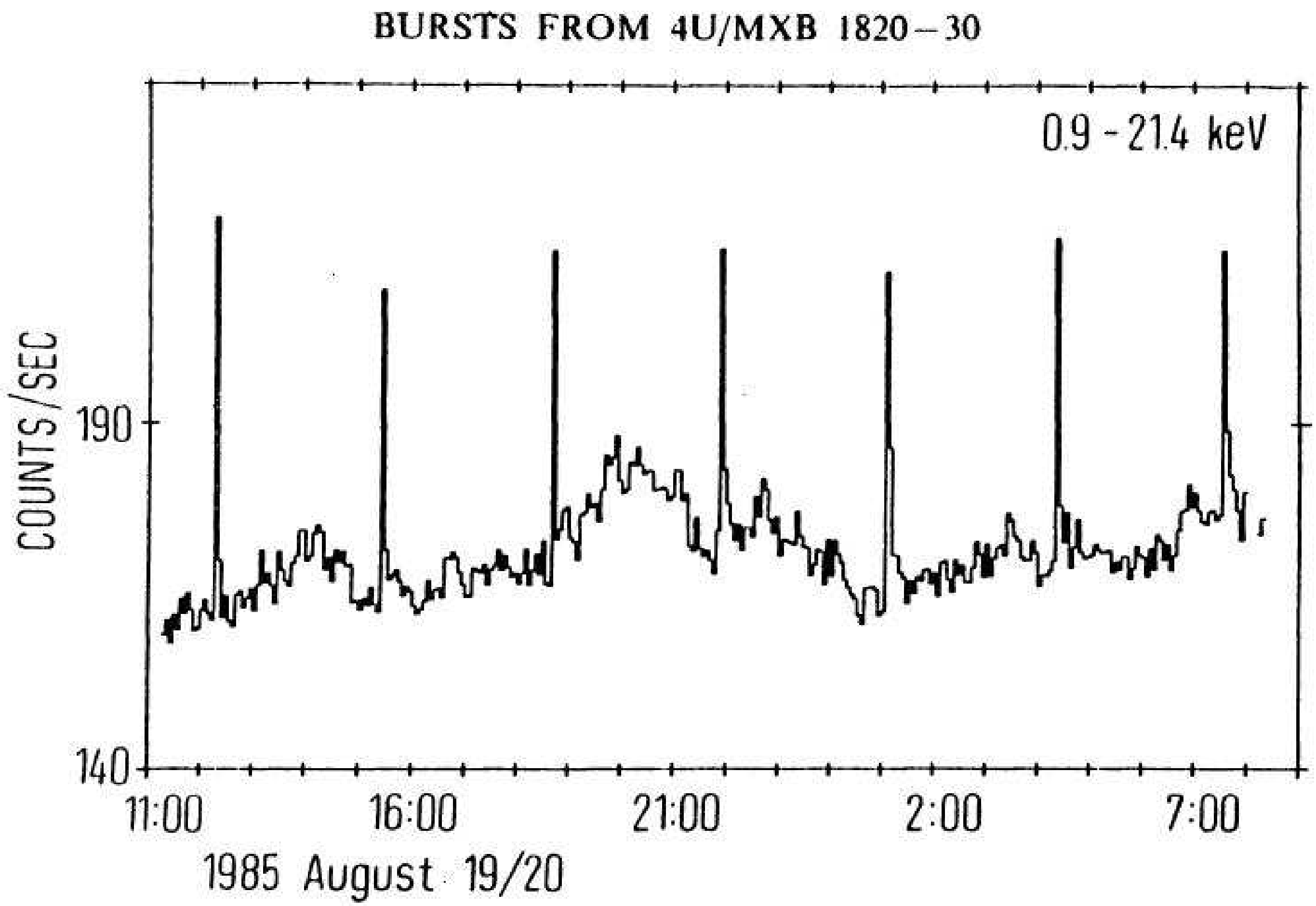

(Lewin, van Paradijs & Taam, 1993, Fig. 3.14b)

Bursts sometimes appear to be regular . . . (burst separations down to 10 min are possible).

X-Ray Bursts

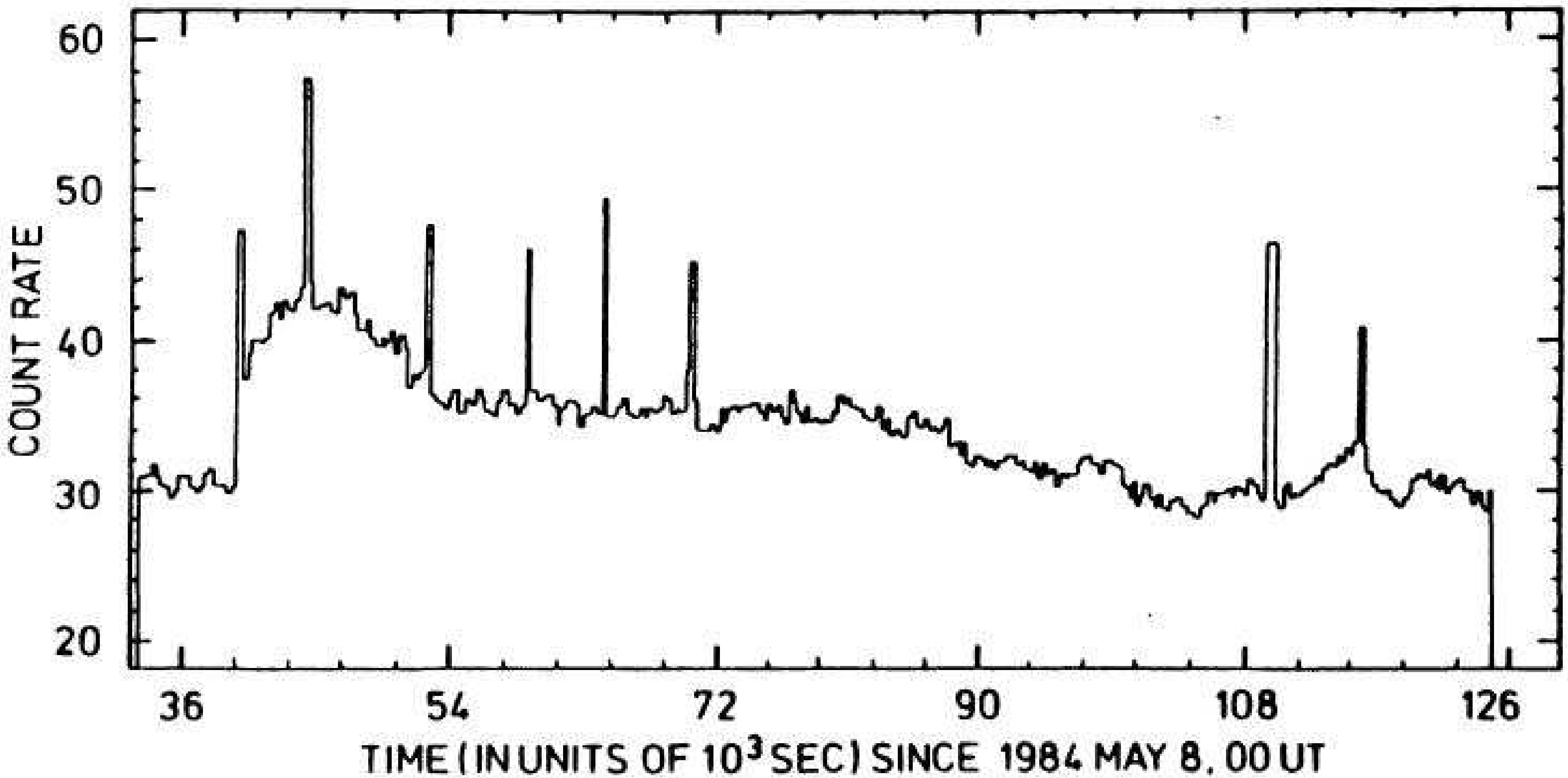

(Lewin, van Paradijs & Taam, 1993, Fig. 3.14b)

. . . and sometimes not.

X-Ray Bursts

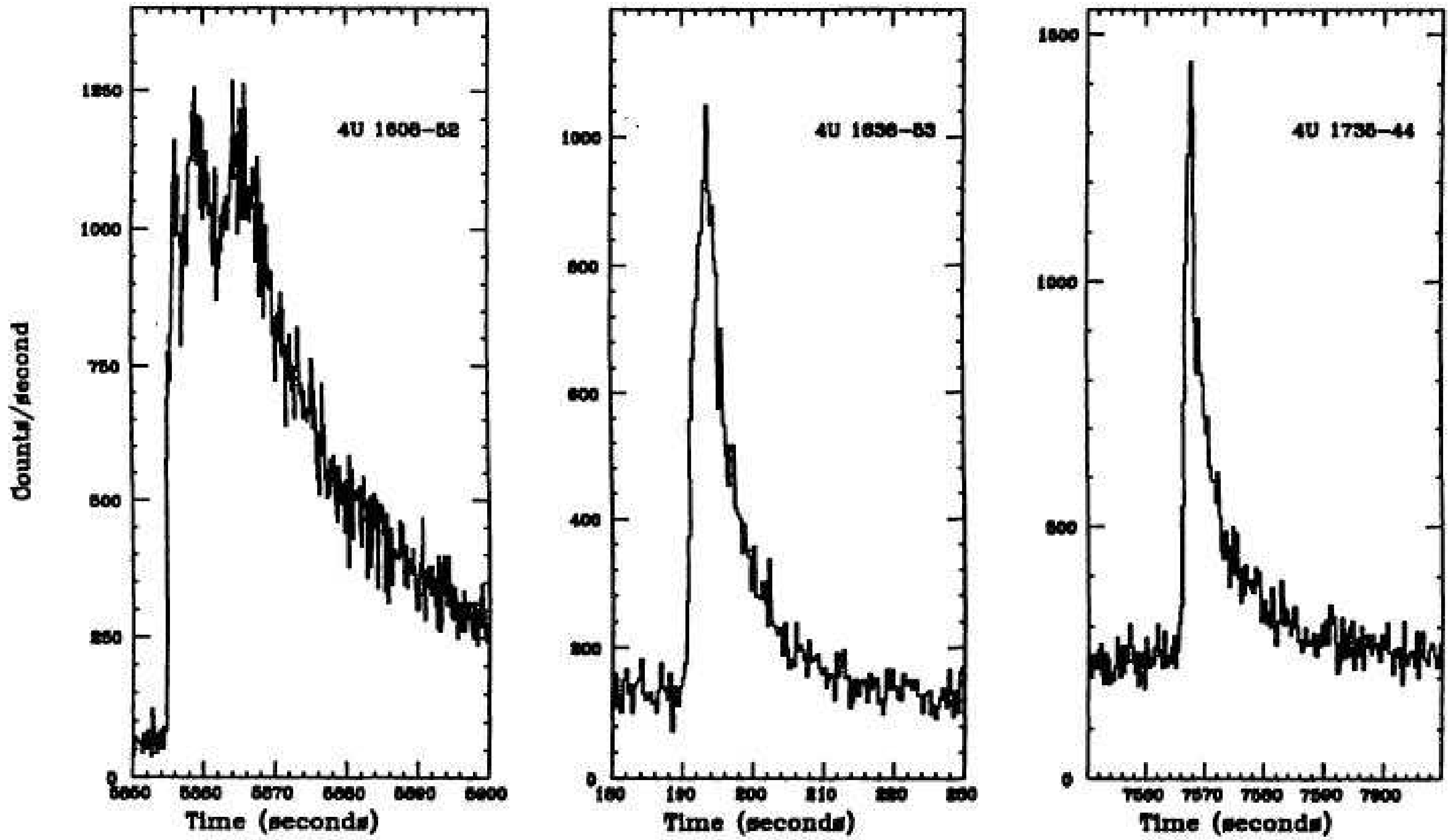

(Lewin, van Paradijs & Taam, 1993, Fig. 3.1)

Bursts come in different shapes, but approximately look like a “FRED”

FRED=Fast Raise and Exponential Decay

X-Ray Bursts

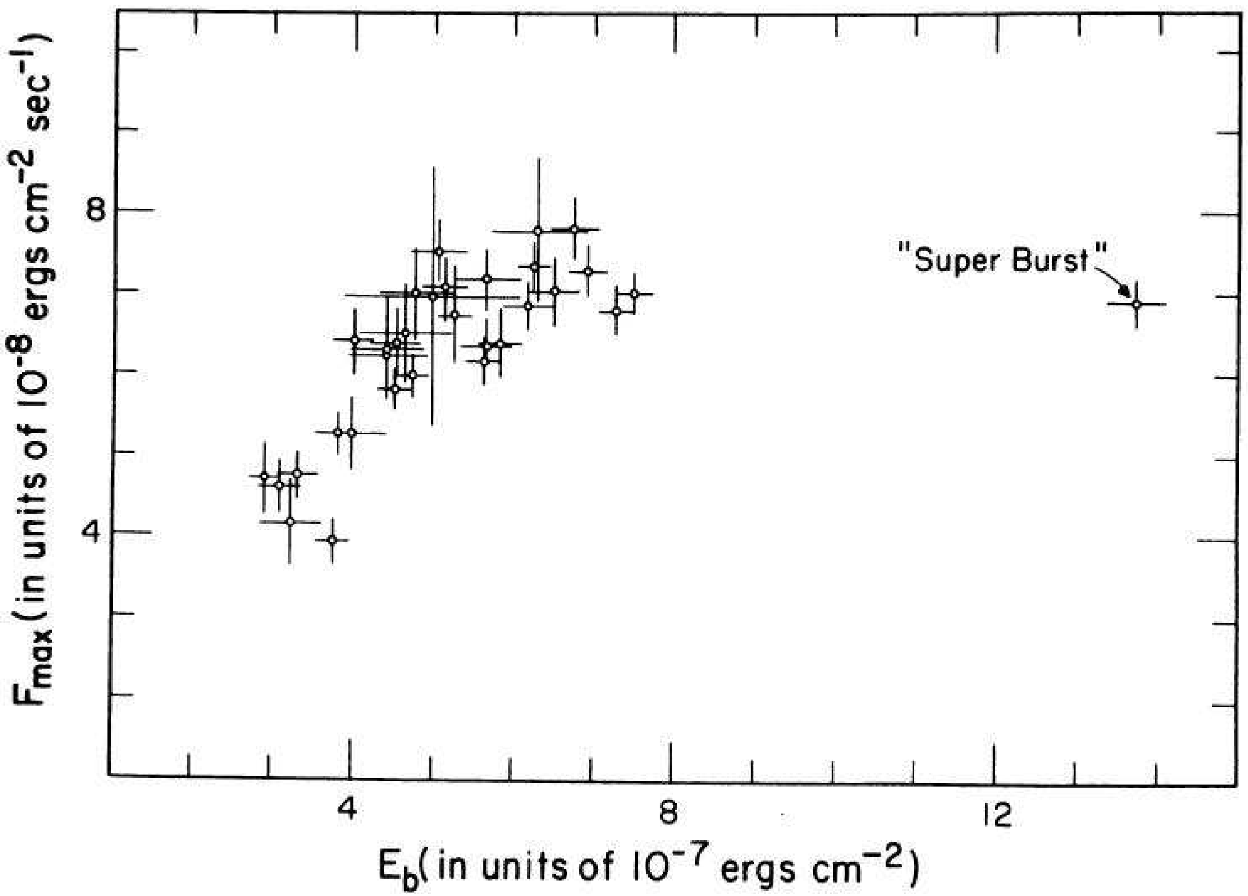

(1728−337; Lewin, van Paradijs & Taam, 1993, Fig. 3.5b)

Peak flux and total fluence of bursts are approxmately linearly correlated

$\Longrightarrow$ more energetic bursts are brighter

X-Ray Bursts

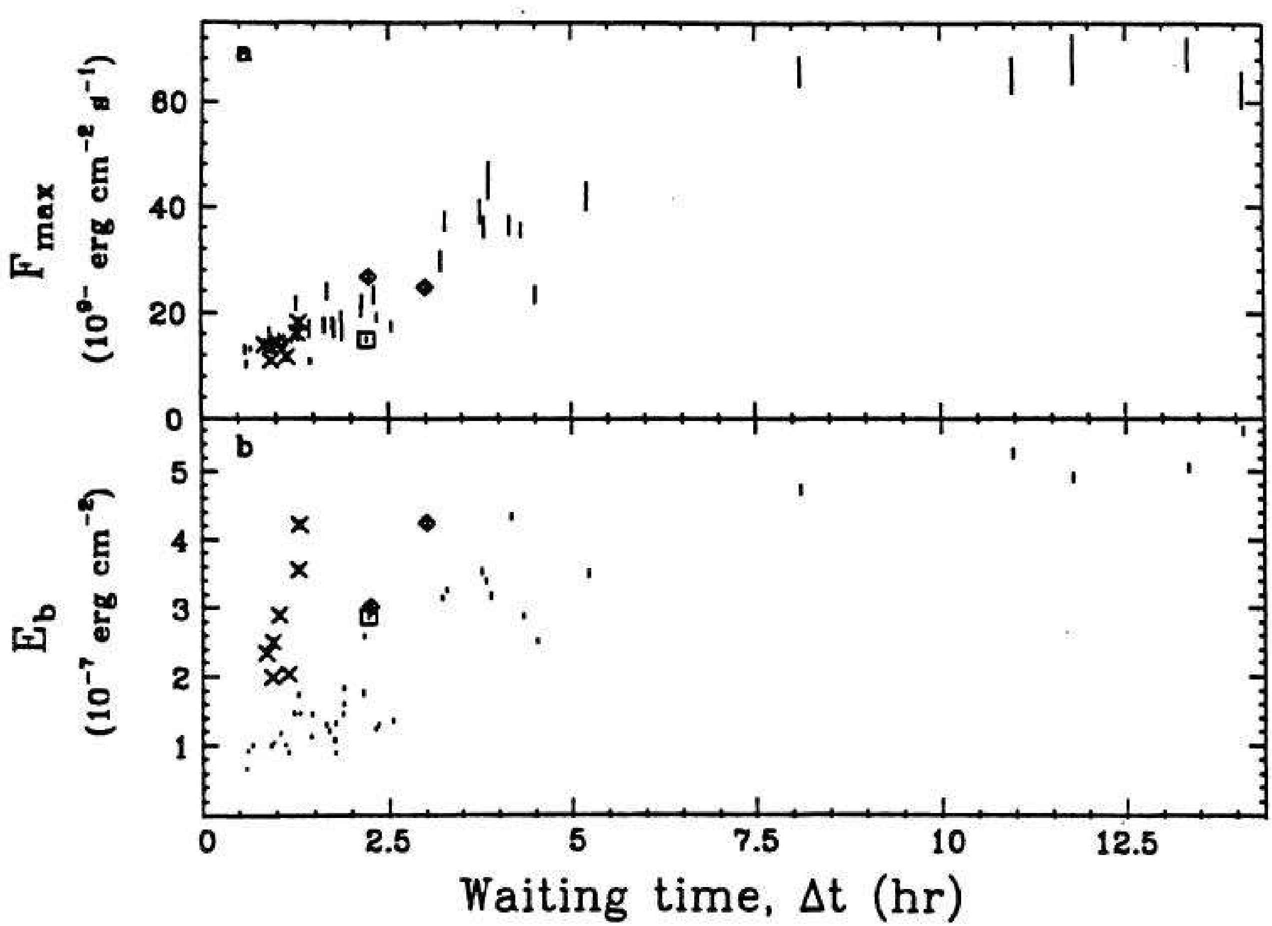

(1636–536; Lewin, van Paradijs & Taam, 1993, Fig. 3.15)

Waiting time and total fluence of bursts are approxmately correlated

$\Longrightarrow$ more energetic bursts come after longer waiting times

X-Ray Bursts

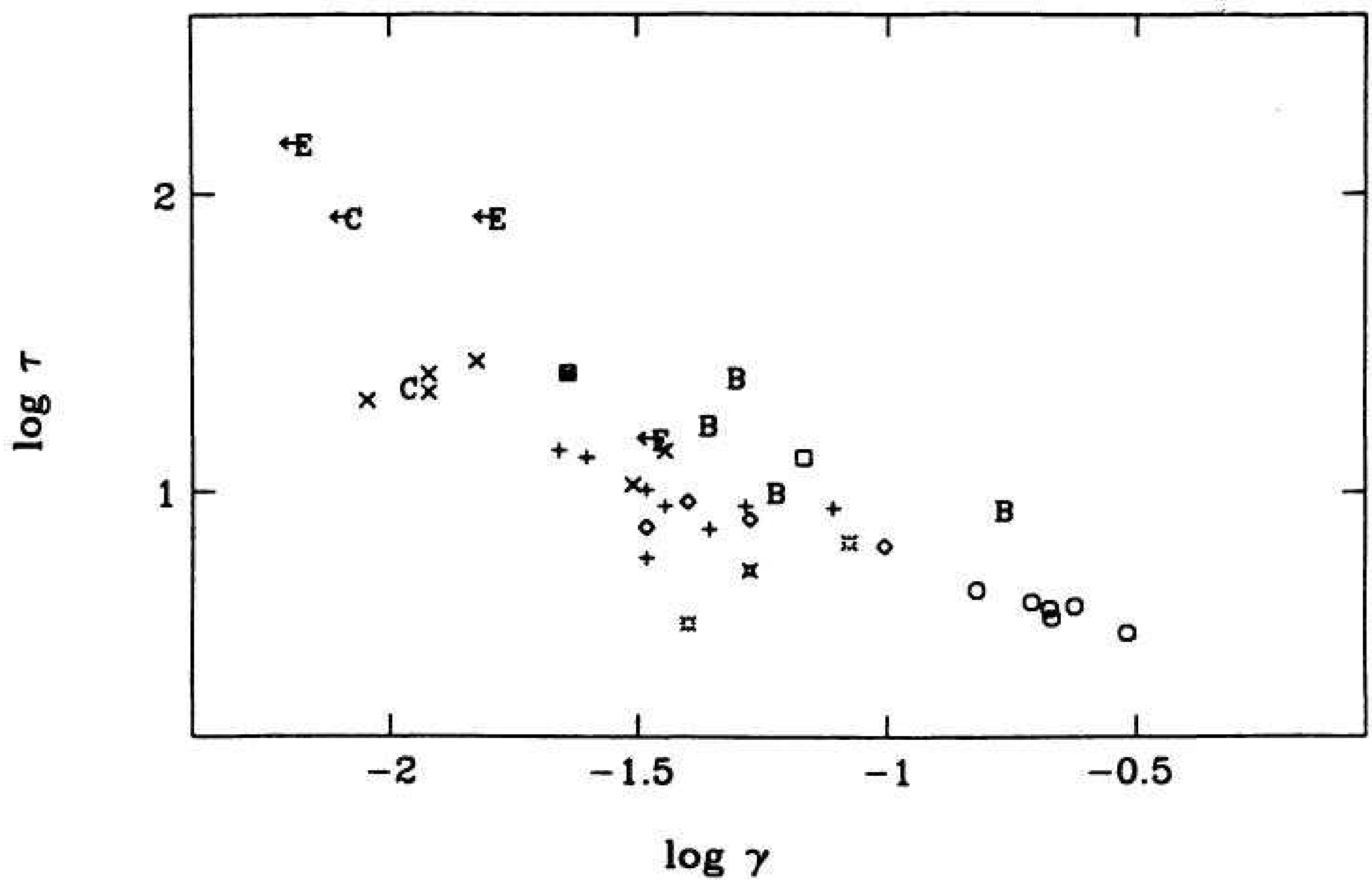

($\gamma = L_{\text{X}}/L_{\text{Edd}}$; Lewin, van Paradijs & Taam, 1993, Fig. 3.17)

Waiting times are longer for low luminosity systems, i.e., lower $\dot{M}$.

X-Ray Bursts

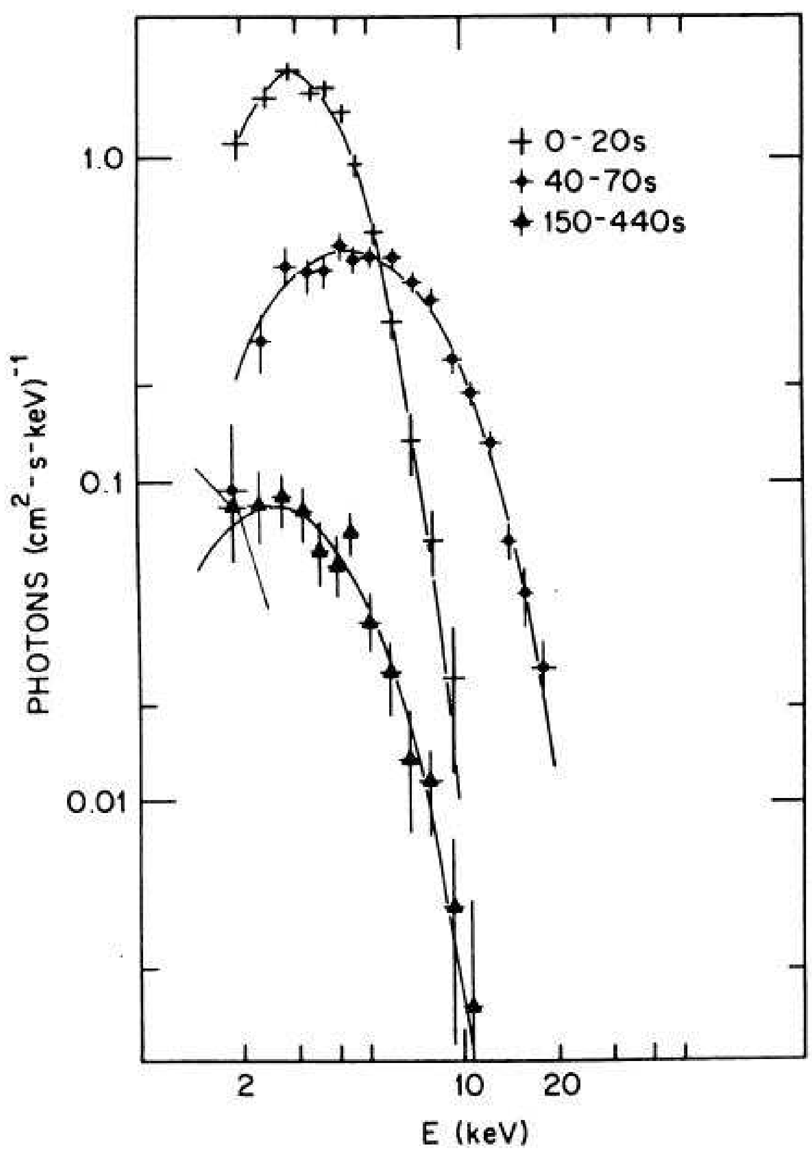

Swank et al. (1977): Spectral shape during the bursts can be well described by a black body spectrum with $kT \sim$ few keV.

$\Longrightarrow$ Optically thick plasma in thermodynamic equilibrium

X-Ray Bursts

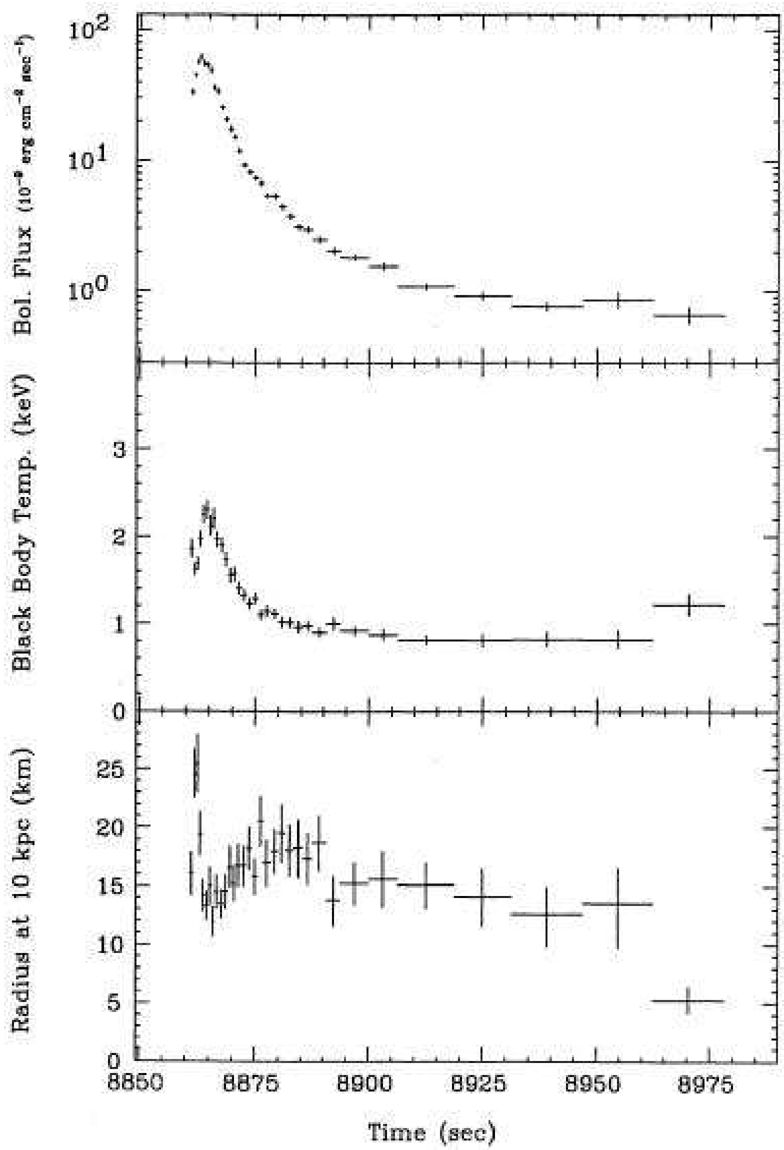

(Lewin, van Paradijs & Taam, 1993, Fig. 3.10)

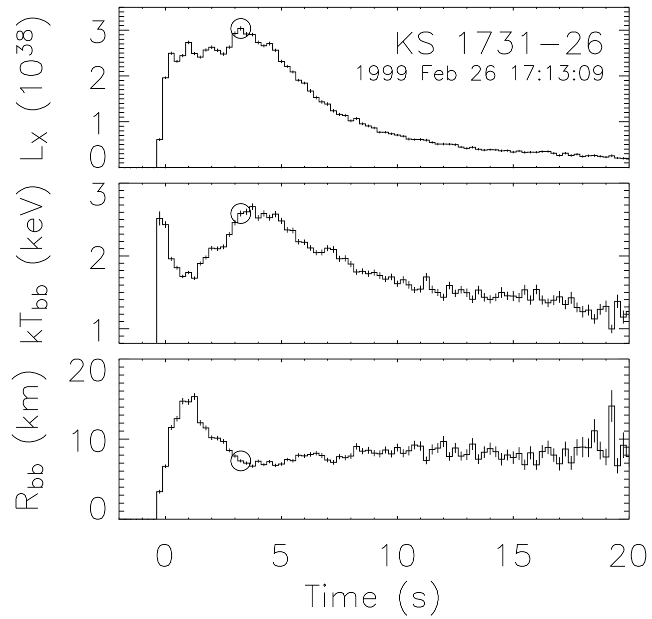

(Galloway et al., 2006, Fig. 1)

Luminosity of a black body: $L_{\mathrm{bb}} = R_{\mathrm{bb}}^2 \sigma T_{\mathrm{bb}}^4$

$\Longrightarrow$ can measure radius of emitter!

$$R = d\sqrt{\frac{4\pi F}{\sigma T^4}}$$

where d estimated distance and F measured flux.

X-Ray Bursts

When looked at in more detail, measuring the temperature during the burst is more complicated:

1. Neutron star is compact, so radiation from surface suffers a gravitational redshift:

$$T_{\text{surface}} = T_{\text{obs}}(1+z) \quad \text{where} \quad 1+z = \left(1 - \frac{2GM}{Rc^2}\right)^{-1/2} \tag{6.3}$$

2. Neutron star atmosphere hardens the surface spectrum through Compton scattering:

$$I_{\text{obs}}(E_{\text{em}}) = B(E_{\text{em}}; T_{\text{eff}})/f^4 \quad \Longleftrightarrow \quad T_{\text{surface}} = fT_{\text{eff}} \tag{6.4}$$

where $B(E,T)$: Black Body spectrum and where

$$f = 1.34 + 0.25((1+X)/1.7)^{2.2}(T_{\text{eff}}/10^7\,\text{K})^4(g/10^{13}\,\text{cm}\,\text{s}^{-2})^{-2.2} \tag{6.5}$$

with $g = (1+z)\cdot GM/R^2$ a correction factor for the surface gravity and $X \sim 0.7$ the atmospheric H-fraction.

Burst Theory, I

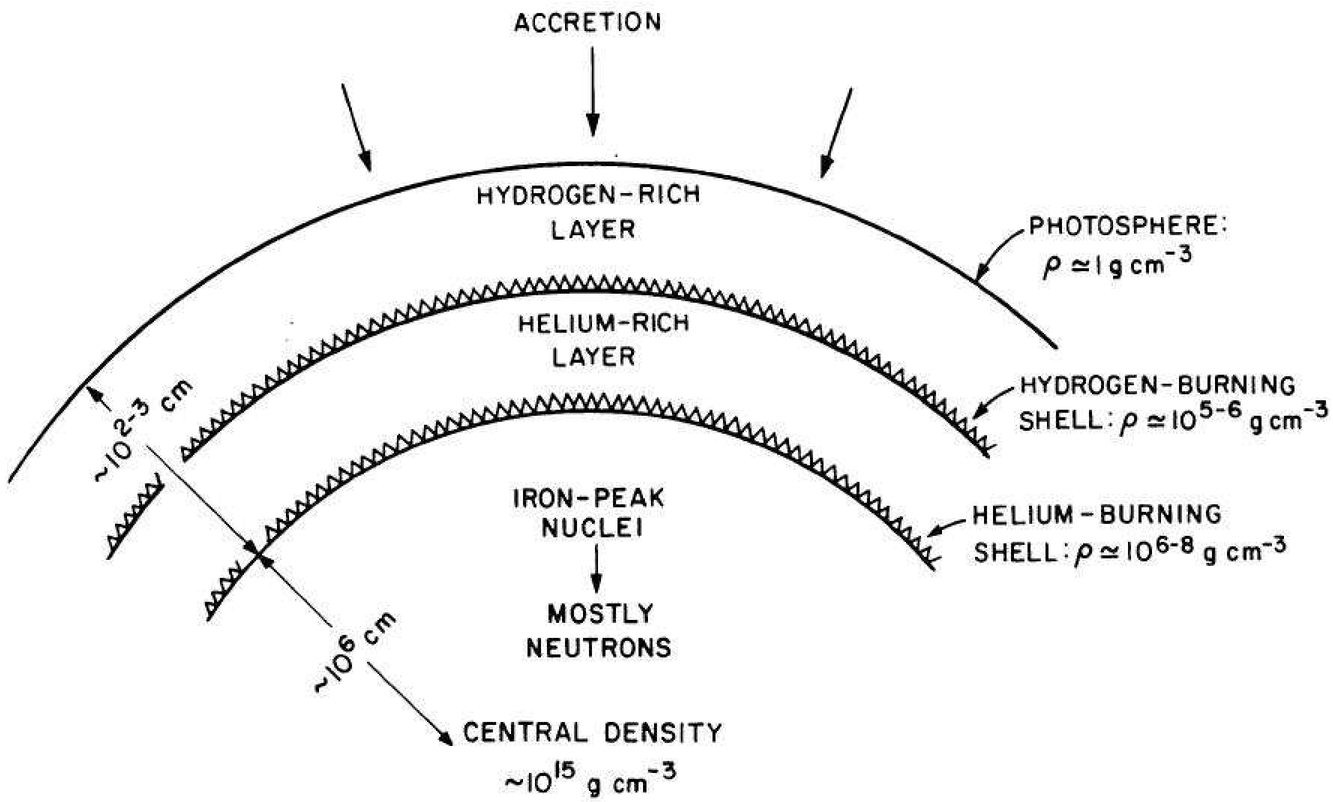

(Joss & Rappaport, 1984, Fig. 13)

Explanation: Bursts are thermonuclear explosions on neutron star surface.

Accretion of hydrogen onto surface $\Longrightarrow$ H fuses into He (mainly electron captures), nuclear statistical equilibrium below that $\Longrightarrow$ He shell, and then higher

Burst Theory, II

Since $T > 10^7$ K: H-burning occurs via the CNO-cycle.

CNO cycle is saturated at $T \gtrsim 8 \times 10^7$ K:

timescale for proton capture $<$ β-decays of standard CNO-cycle

$t_{1/2} \sim$ 100–1000 s for ^{13}N, ^{14}O, ^{15}O)

$\Longrightarrow$ "hot CNO cycle":

$$^{12}\mathrm{C}(p,\gamma)^{13}\mathrm{N}(p,\gamma)^{14}\mathrm{O}(\beta^+)^{14}\mathrm{N}(p,\gamma)^{15}\mathrm{O}(\beta^+)^{15}\mathrm{N}(p,\alpha)^{12}\mathrm{C}$$

This process is instable for

$$\dot{m} < 900\,\mathrm{g\,cm^{-2}\,s^{-1}}(Z_{\mathrm{CNO}}/0.01)^{1/2} \tag{6.6}$$

where Z: mass fraction and where $\dot{m} = \dot{M}/(4\pi R^2)$.

$\Longrightarrow$ Type I burst

Burst Theory, III

For higher $\dot{m}$: H-burning is stable. But: ρ is high, so He burning is also possible (mainly 3α process):

- For $\dot{m} < 2000\,\mathrm{g\,cm^{-2}\,s^{-1}}(Z_{\mathrm{CNO}}/0.01)^{13/18}$:
  H burns faster than He, $\Longrightarrow$ pure He X-ray bursts
- Above this $\dot{m}$: simultaneous H/He-burning.
  Because of the strong temperature dependence of the 3α process:
  – For $T < 5 \times 10^8\,\mathrm{K}$: He ignites explosively in thin shell $\Longrightarrow$ X-ray burst
    conditions typically ok for explosive energy release, once 10^{21} g material have been accumulated; for $\dot{M} \sim 10^{17}\,\mathrm{g\,s^{-1}}$ this corresponds to burst recurrence timescales of 10000 s, as observed; energy release $\sim 10^{39}\,\mathrm{erg\,s^{-1}}$
  – For $T > 5 \times 10^8\,\mathrm{K}$: H and He burns stable
    $\Longrightarrow$ no bursts in higher $\dot{M}$ sources!

see Strohmayer & Bildsten (2006) for recent review and references to current ideas. Early theory (more understandable): Hansen & van Horn (1975), Lamb & Lamb (1978), Taam & Picklum (1979)

Burst Theory, IV

The Energy released during the burst is:

$$E_{\text{burst}} = Q\frac{4\pi R^2 H\rho}{m_{\text{H}}} \sim 2 - 8 \times 10^{39}\,\text{erg} \tag{6.7}$$

where typical parameters are $R = 10\,\text{km}$, $H \sim 10^2\,\text{cm}$, $\rho = 10^6\,\text{g}\,\text{cm}^{-3}$, and

- H-burning: $Q = 7\,\text{MeV}\,\text{nucleon}^{-1}$
- He-burning: $Q = 1.5\,\text{MeV}\,\text{nucleon}^{-1}$

If the whole accreted matter $M_{\text{acc}} = 4\pi R^2 H\rho$ is used, then the time averaged burst luminosity is

$$L_{\text{burst}} = \frac{E_{\text{burst}}}{\Delta t} = Q\frac{\dot{M}}{m_{\text{H}}} \tag{6.8}$$

Since the accretion luminosity is

$$L_{\text{acc}} = \frac{GM\dot{M}}{R} \tag{6.9}$$

the ratio between persistent and burst emission is

$$\alpha = 30 - 120\left(\frac{M}{M_\odot}\right)\left(\frac{R}{10\,\text{km}}\right)^{-1} \tag{6.10}$$

similar to what is observed.

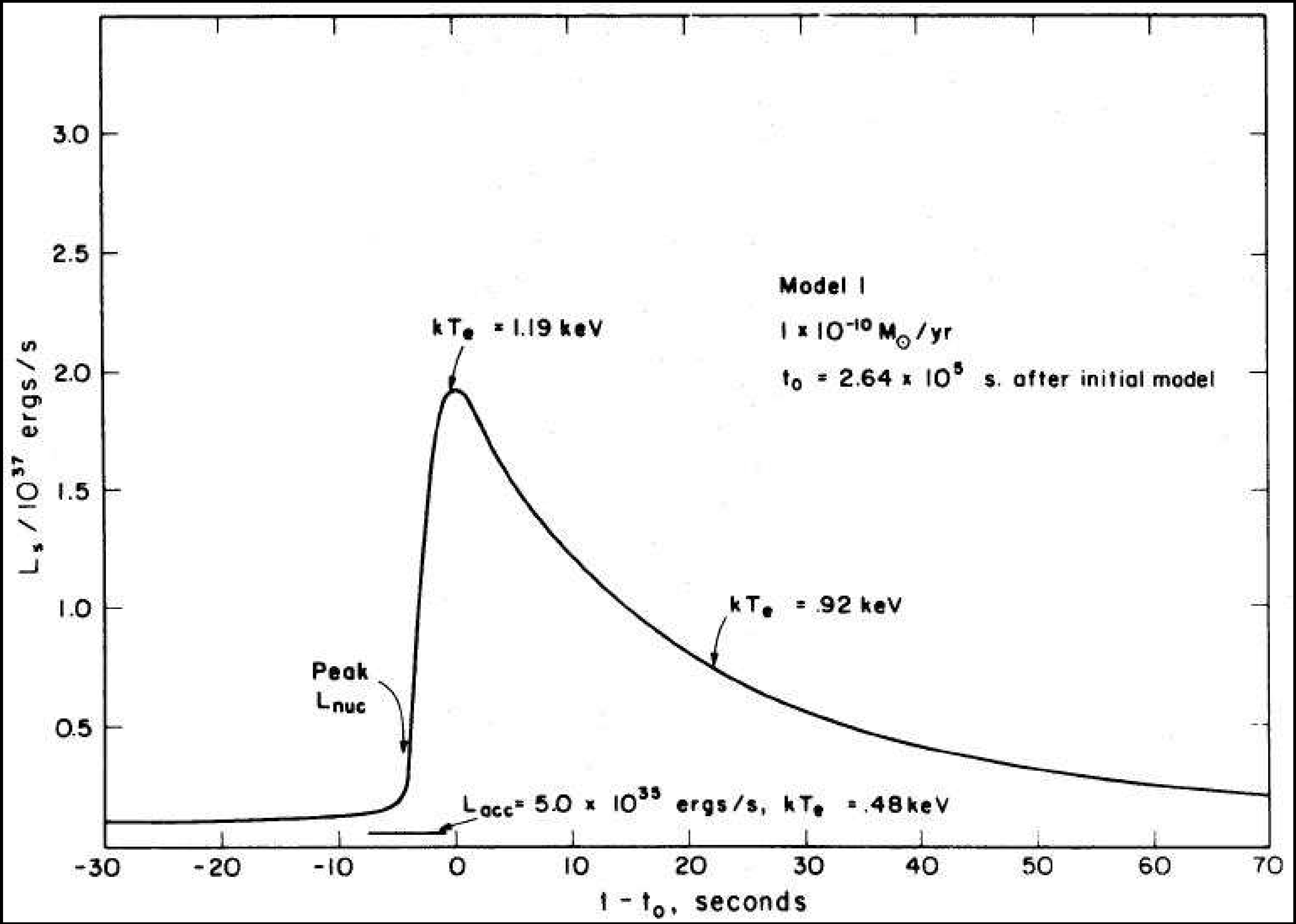

(Taam & Picklum, 1979, Fig. 2)

Theoretical outburst profile

Burst Theory, VI

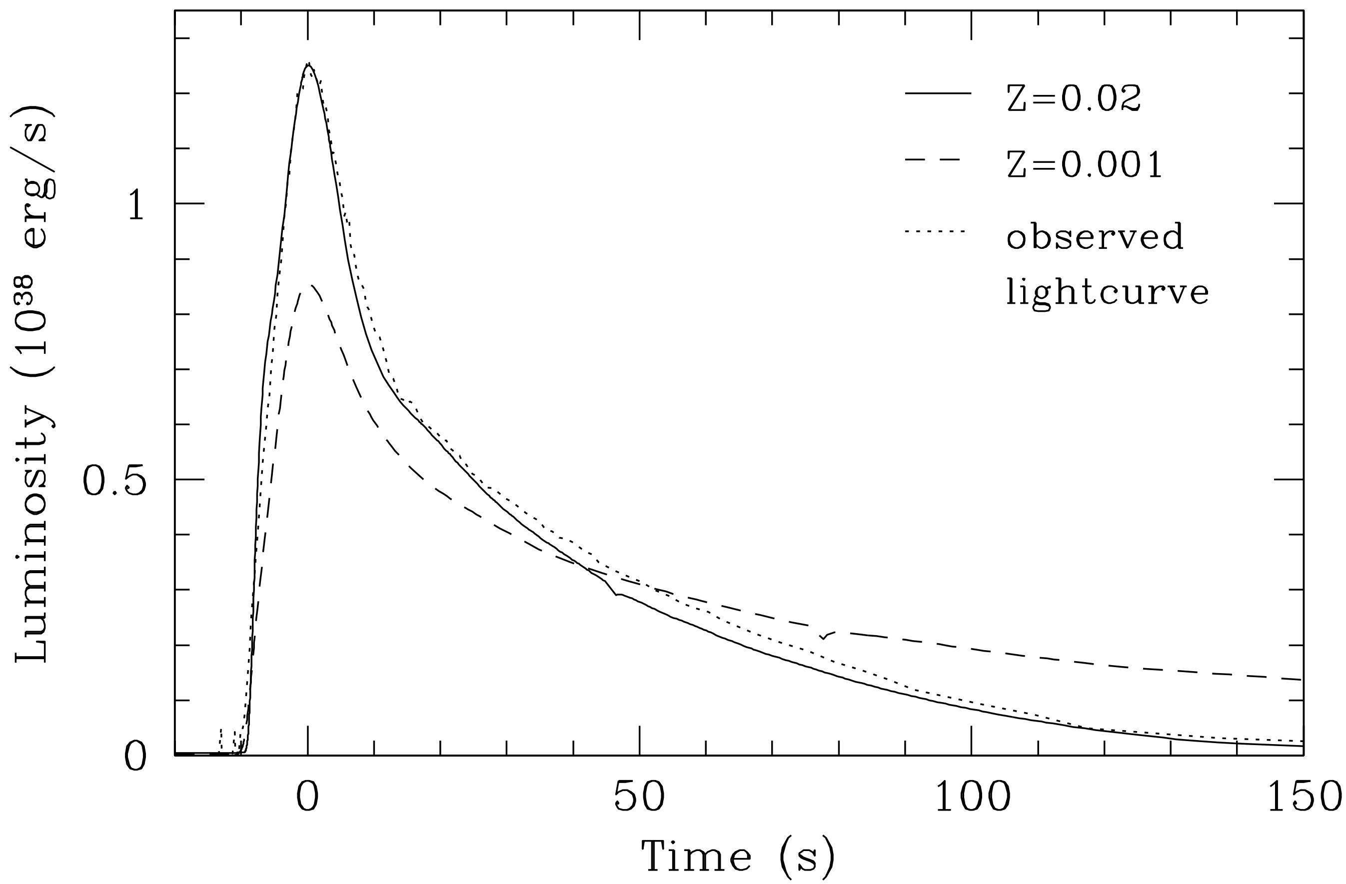

(Cumming, 2004, Fig. 3; calculation for average burst profi le of GS 1826−24, the "clocked burster" with 4 h burst recurrence timescale)

Theory and observations of type I bursts agree well

Burst Theory, VII

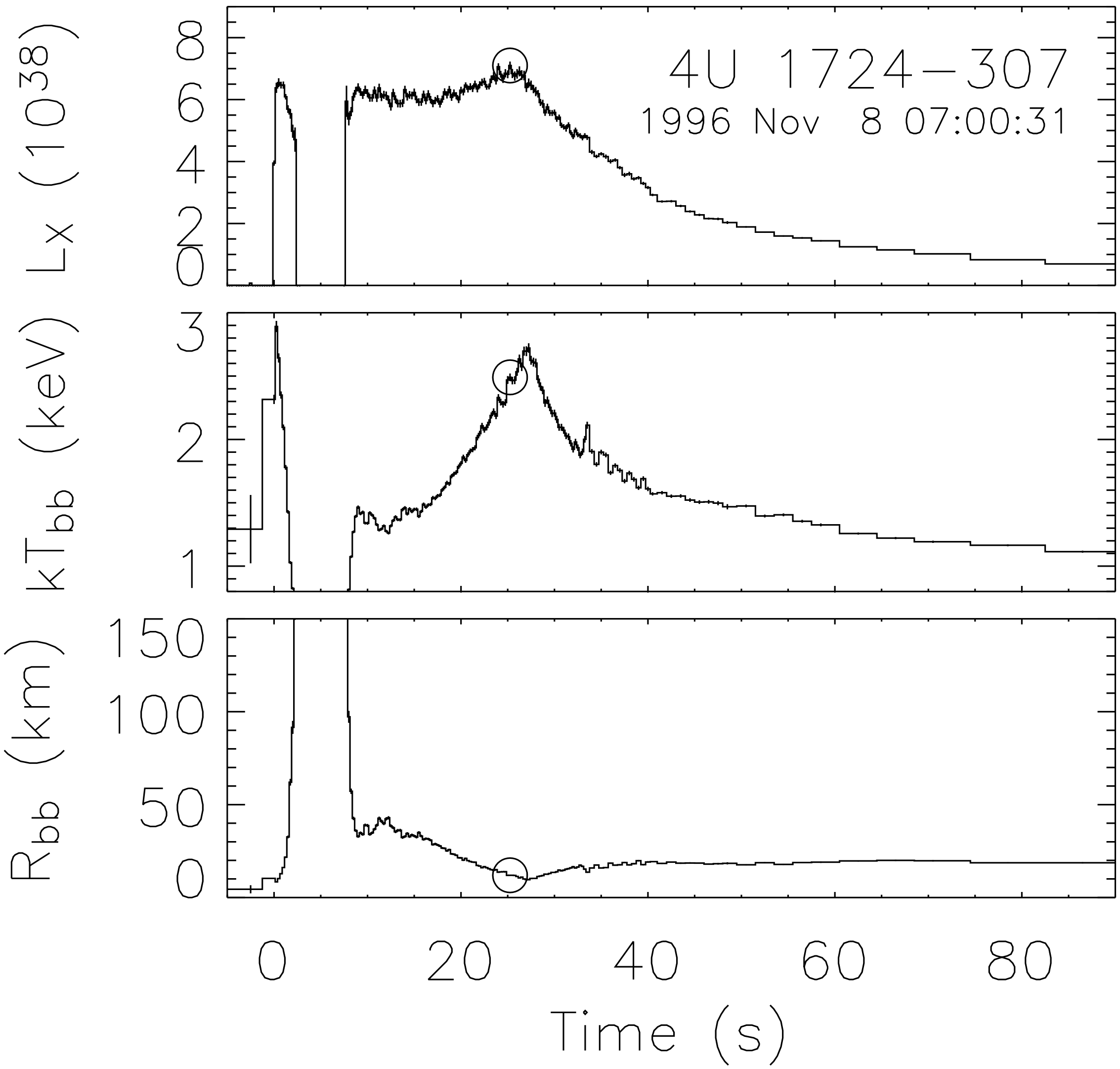

For most luminous bursts (large He fraction):

$L \gtrsim L_{\text{Edd}}$

$\Longrightarrow$ atmosphere "ejected"

$\Longrightarrow$ radius expansion bursts.

Note that outside of bursts $R_{\text{BB}} \sim R_{\text{neutron star}}$!

(Galloway et al., 2006, Fig. 10)

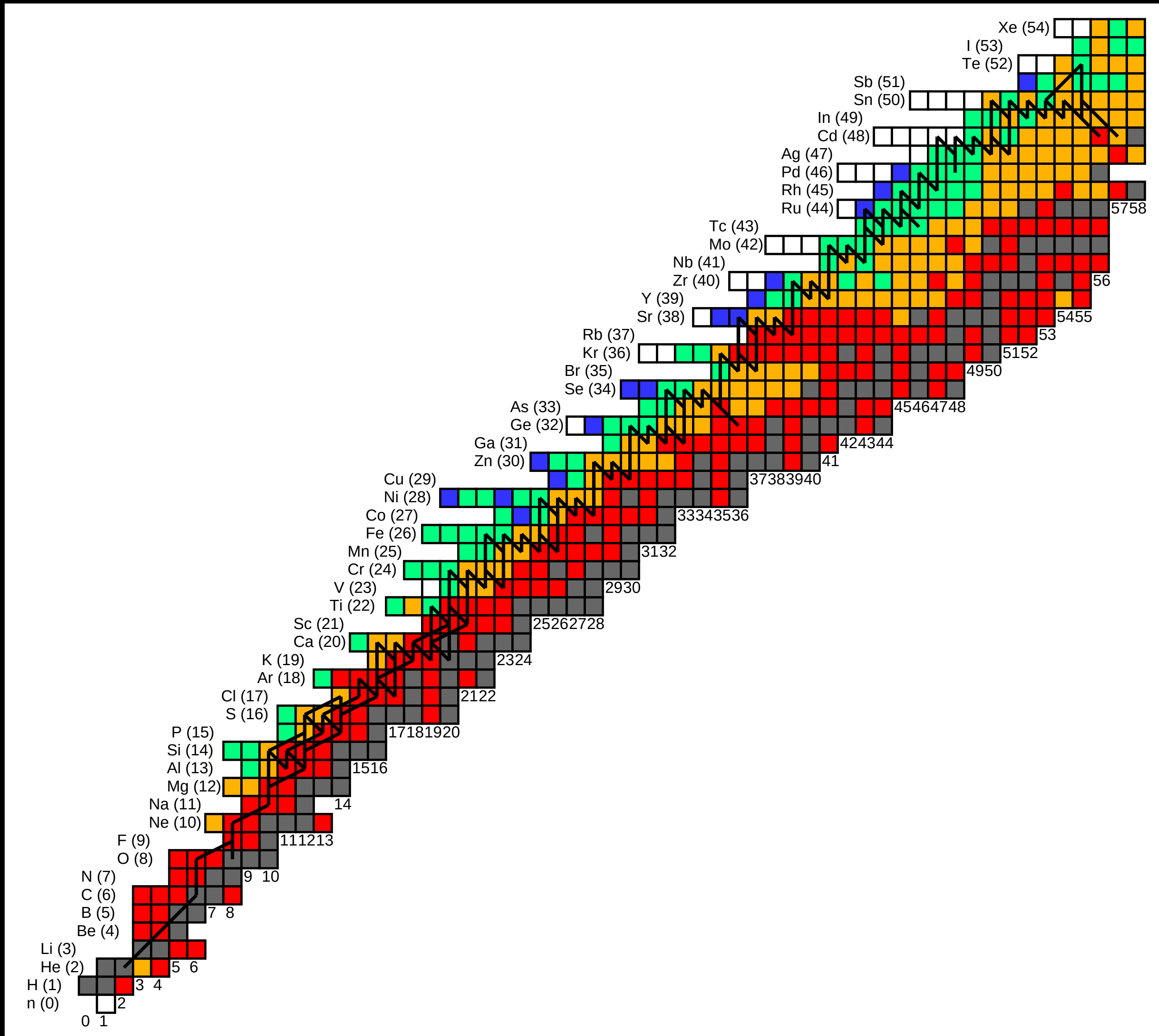

(Schatz & Rehm, 2006, Fig. 1)

For $T \gtrsim 10^9$ K, fusion of higher Z elements is possible during X-ray burst (rp-process)

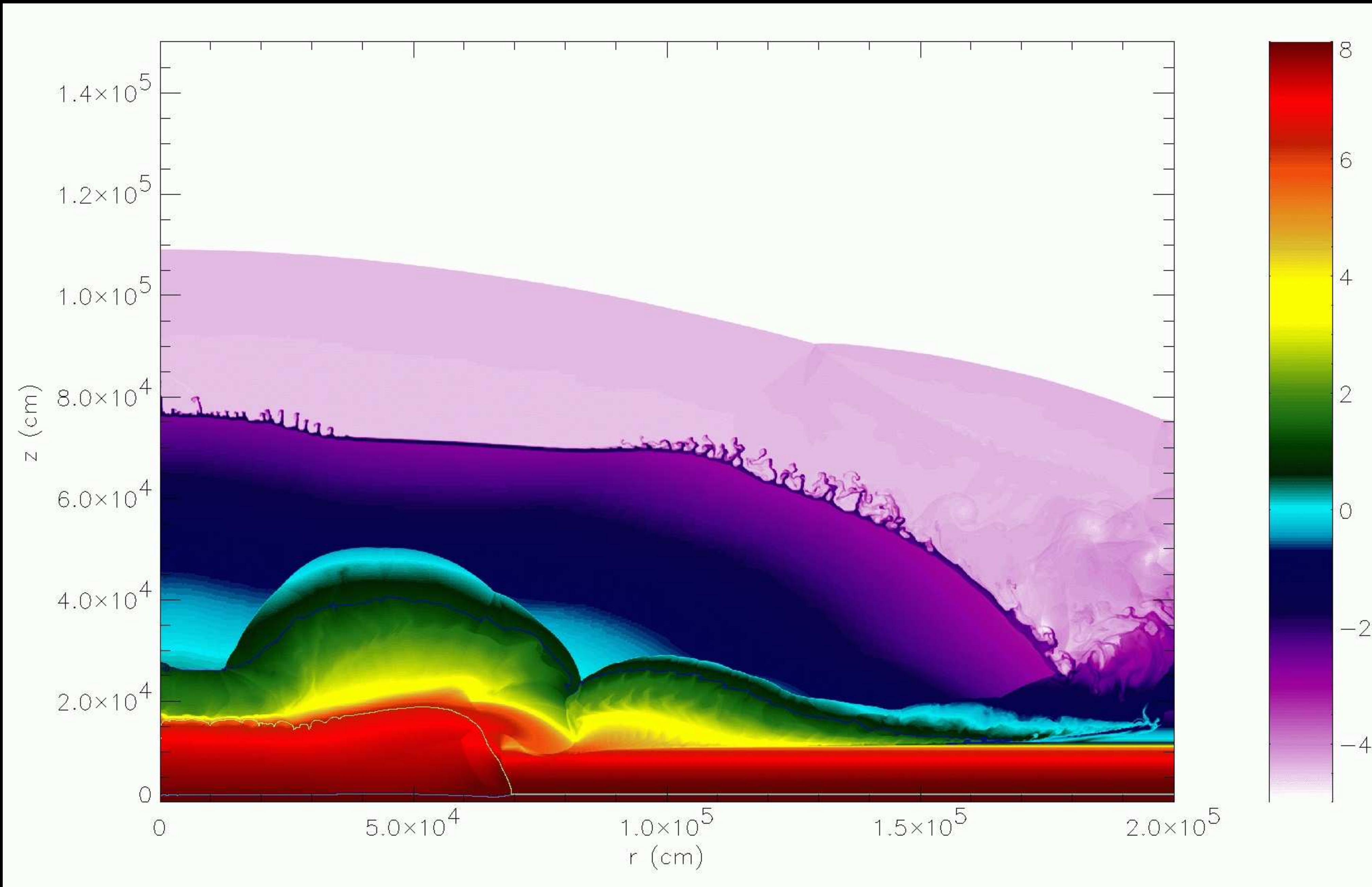

$t = 60\,\mu$s

Zingale et al. (2001): 2D hydrodynamical calculations of He detonation spreading over neutron star

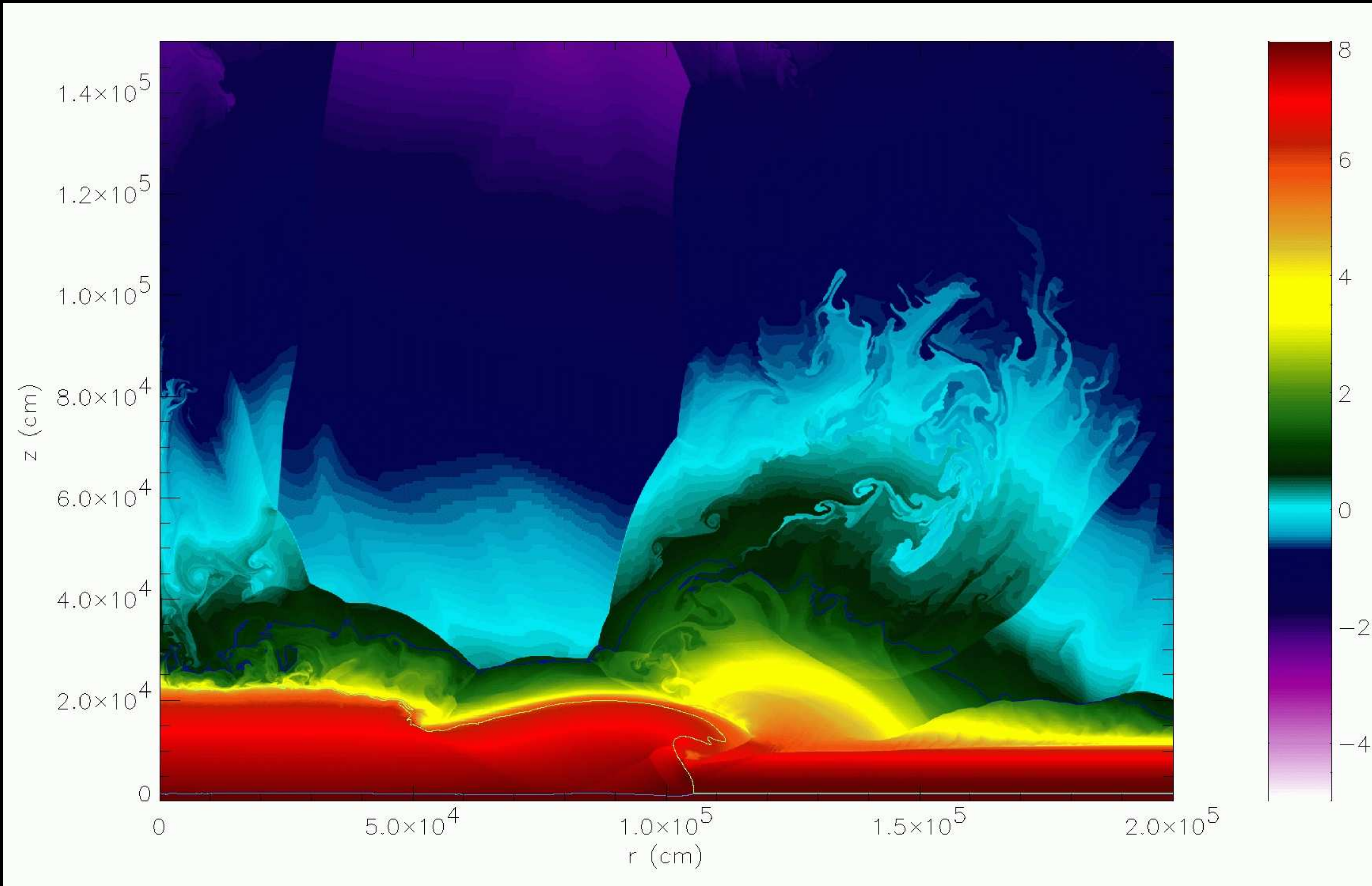

$t = 90\,\mu$s

Zingale et al. (2001): 2D hydrodynamical calculations of He detonation spreading over neutron star

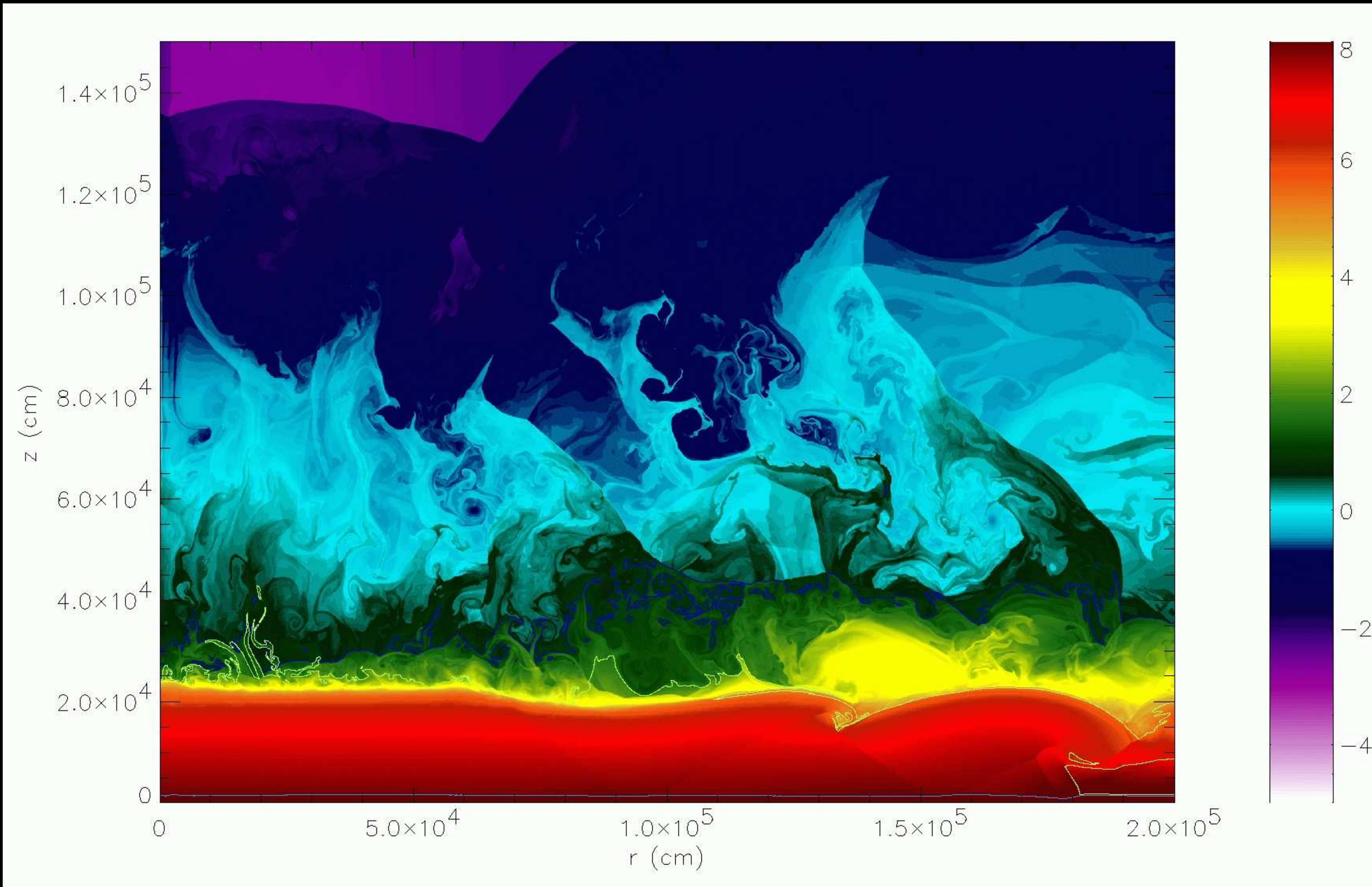

$t = 150\,\mu s$

Zingale et al. (2001): 2D hydrodynamical calculations of He detonation spreading over neutron star

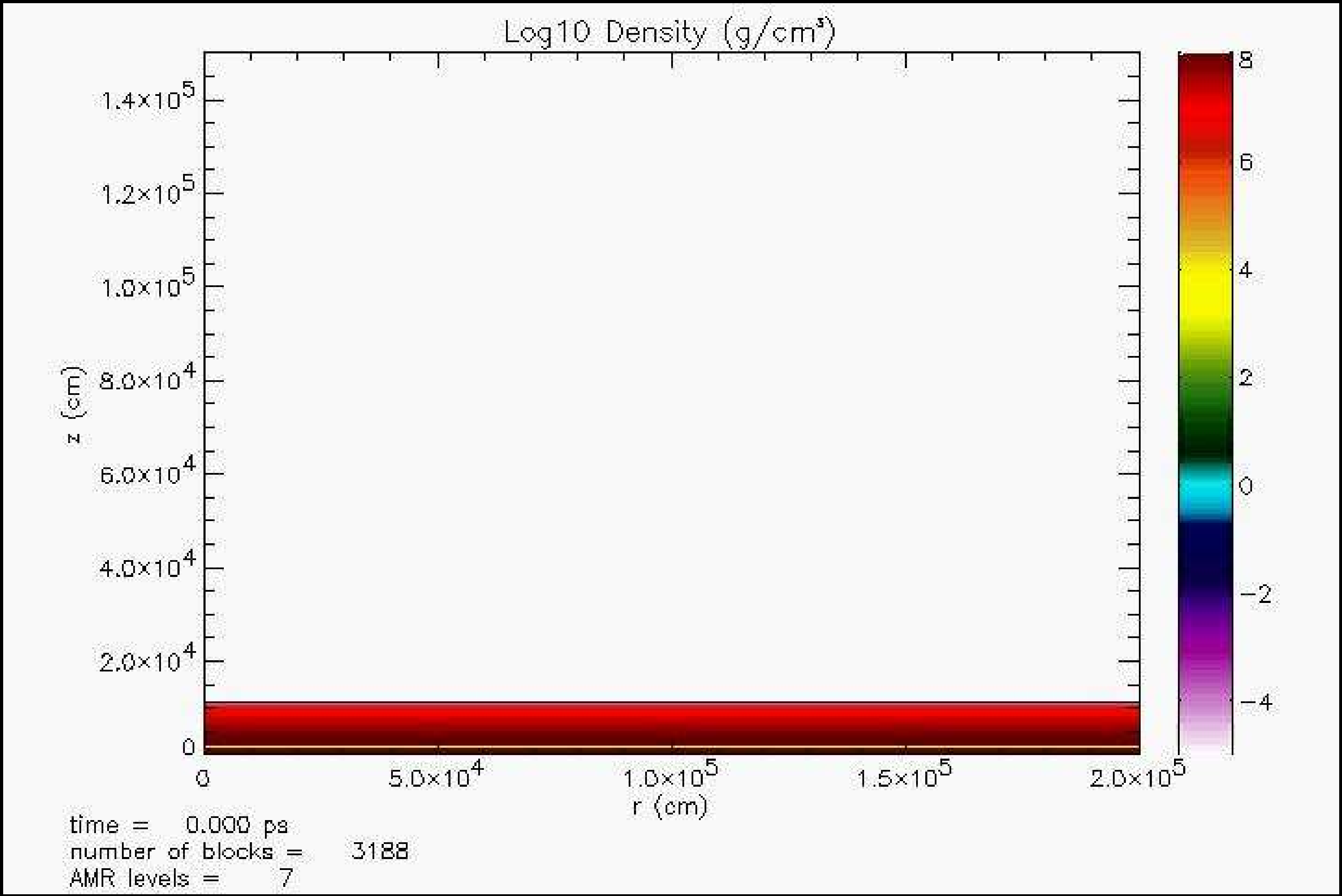

Zingale et al. (2001): Evolution of a burst: density evolution

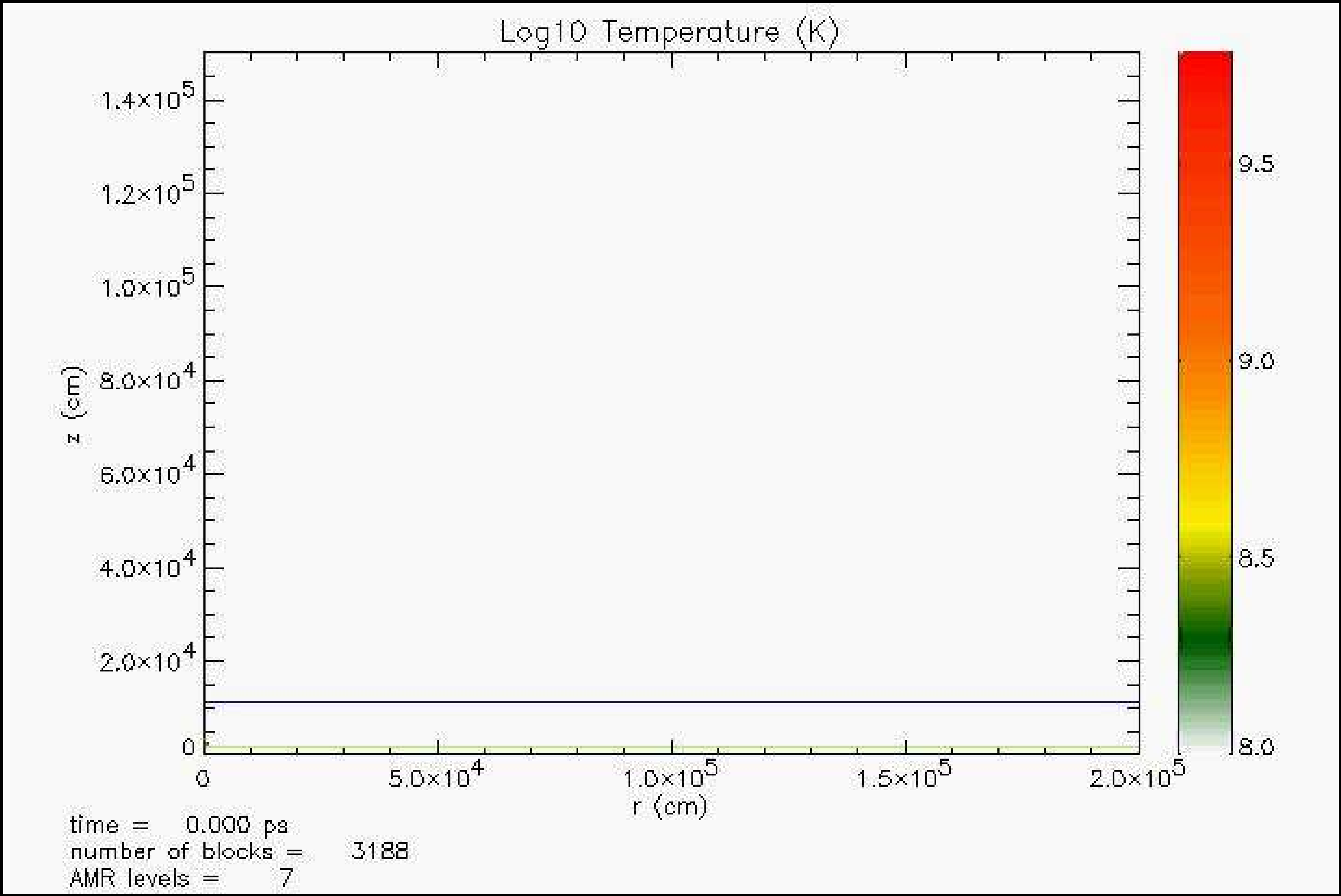

Zingale et al. (2001): Evolution of a burst: temperature evolution

Superbursts, I

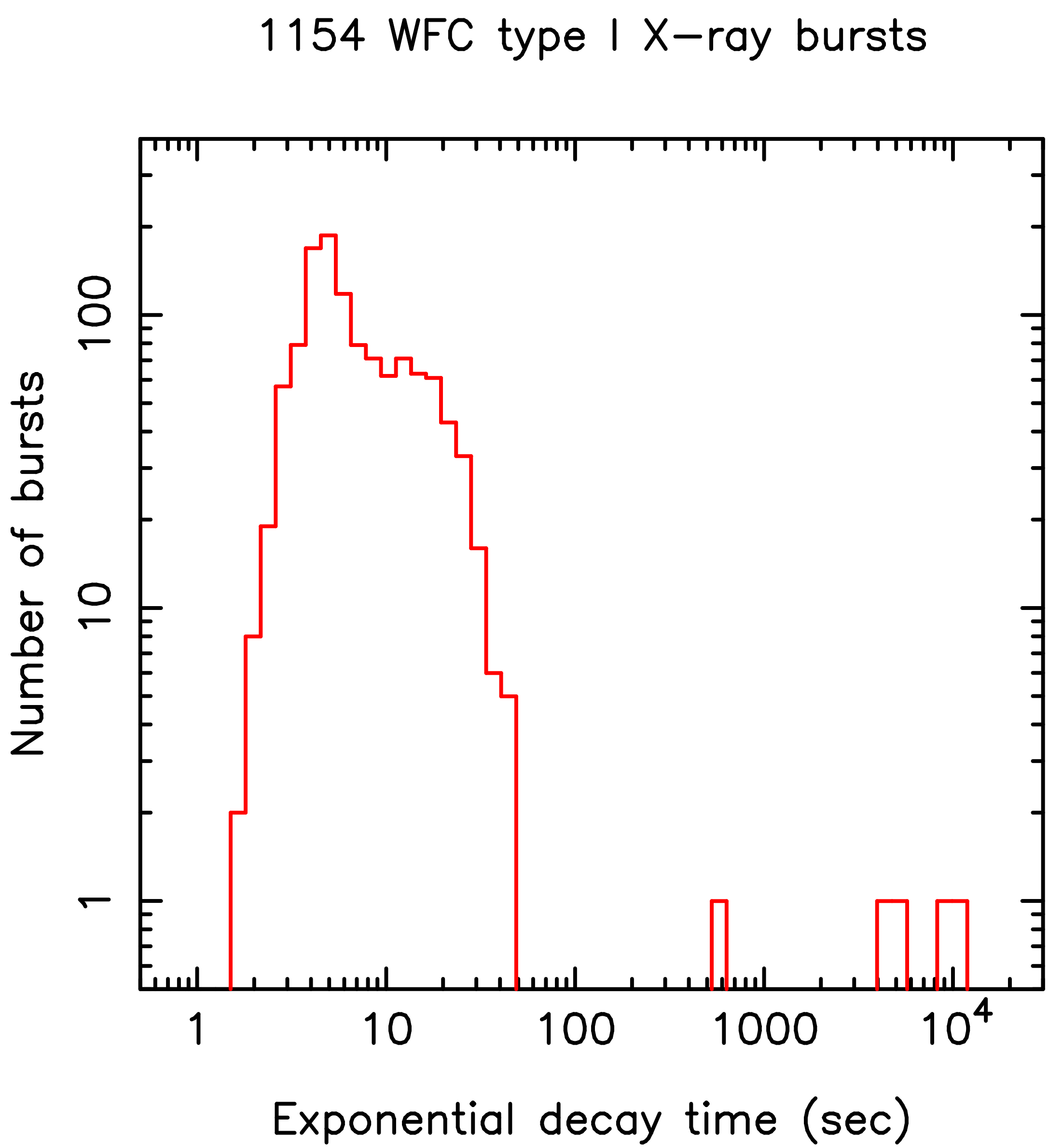

Some bursts have very long duration

(Kuulkers, 2004, Fig. 1)

Superbursts, II

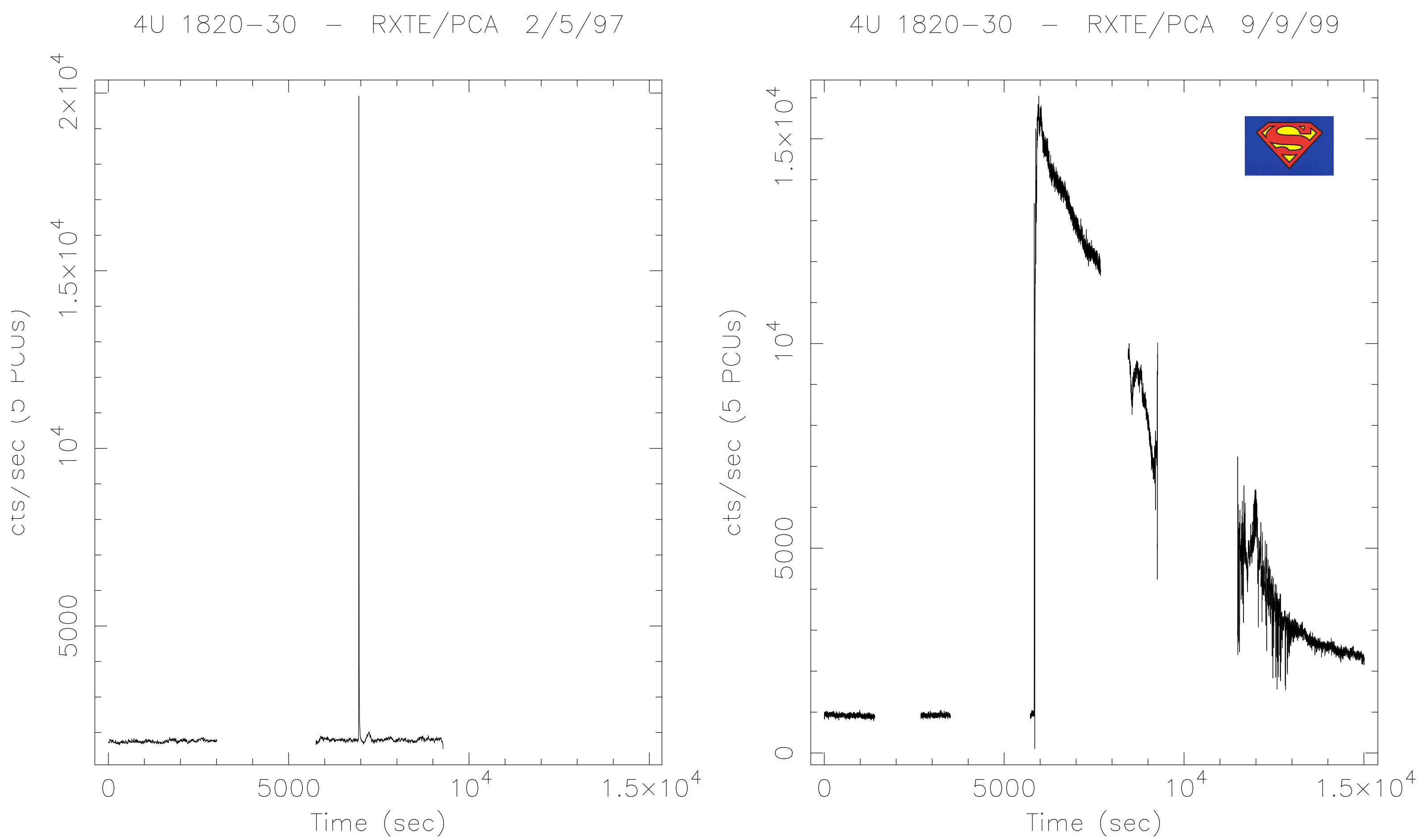

(Kuulkers, 2004, Fig. 3)

Some bursts have very long duration: Superbursts

Superbursts, III

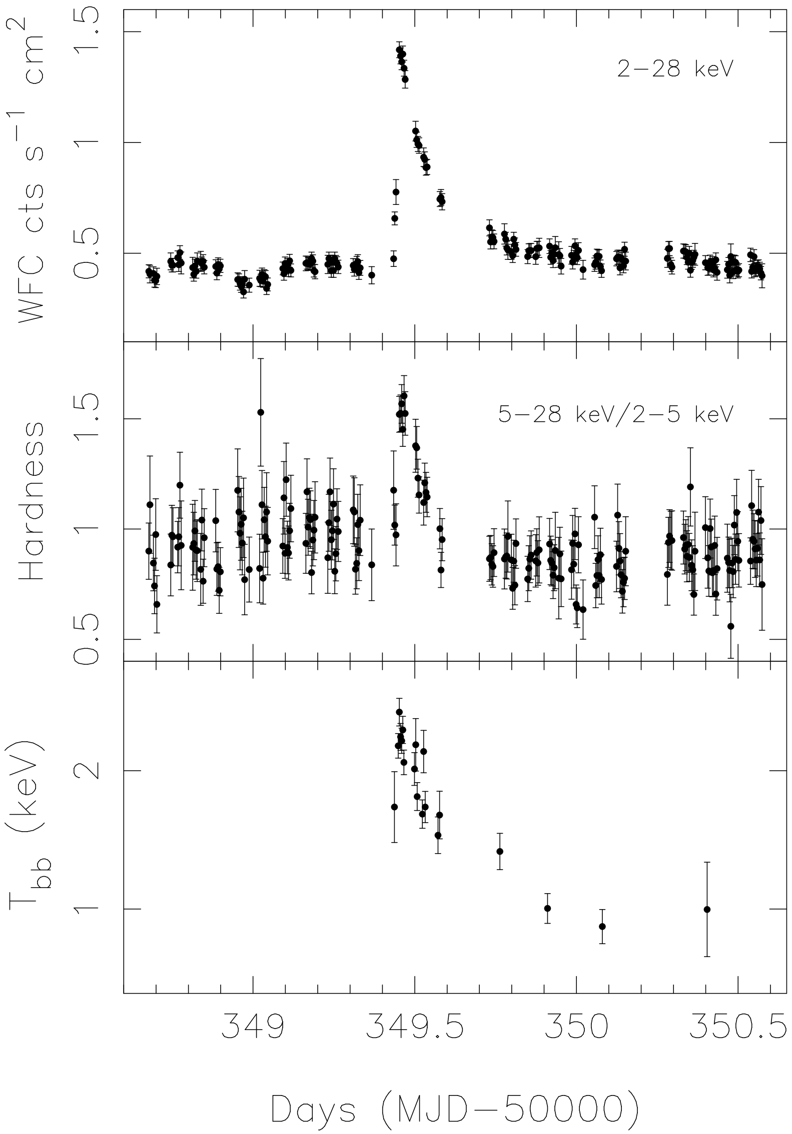

Temperature evolution over the superburst, similar to normal bursts, but the burst takes much longer $\Longrightarrow$ explosive C burning?

But: Early theory: pure ^{12}C layer is very stable, so would expect long recurrence time (100 s of years; Taam & Picklum 1979)

Cumming & Bildsten (2001): better theory: C burning is possible if there is a small ^{12}C fraction ($Z(^{12}\mathrm{C}) \sim 0.1$), so superbursts are probably signs of explosive carbon burning.

(Kuulkers, 2004, Fig. 2)

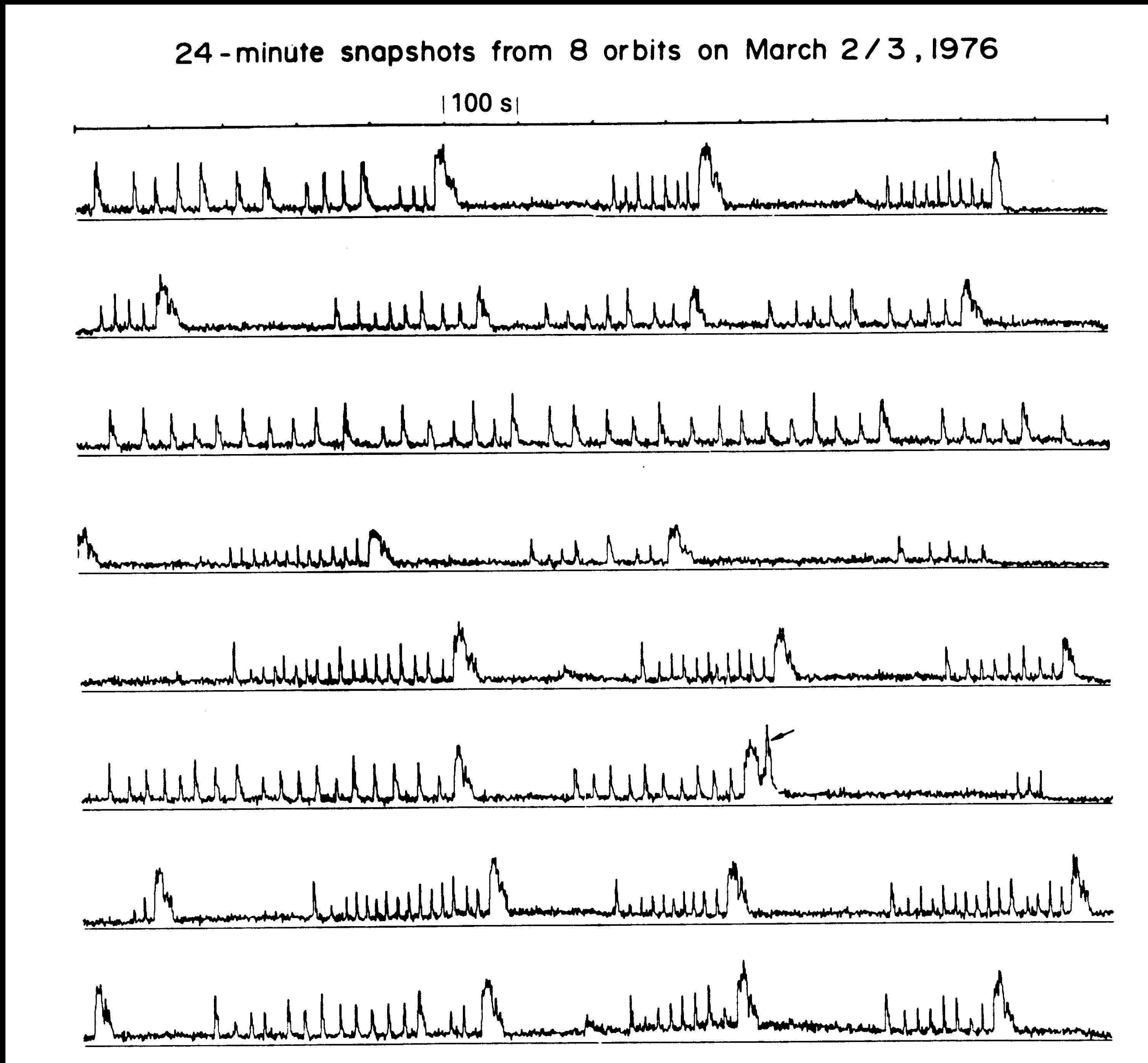

(Joss & Rappaport, 1984, Fig. 18)

Bursting of the "Rapid Burster" MXB1730−335: Type I and Type II bursts.

Type II bursts: magnetospheric gate model: B-field blocks accretion until $P_{\rm gas} > P_{\rm mag} \Longrightarrow$ BOOM.

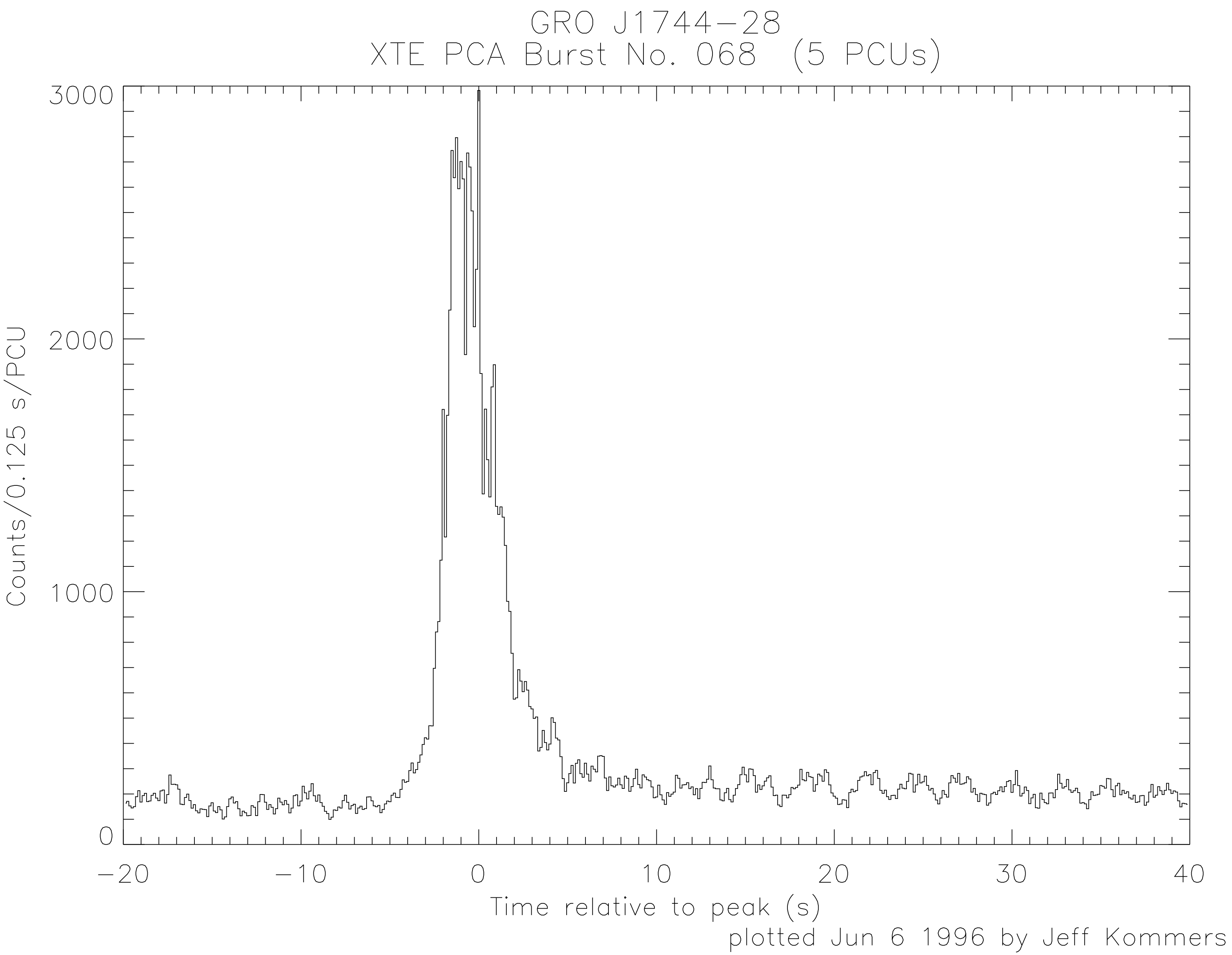

(Bursting Pulsar; Kommers, 1996, priv. comm.)

Before 1995 December 2: X-ray bursts and pulsations cannot occur in the same object.

Then: GRO J1744−28 the bursting pulsar. Pulsations with 2 Hz *and* type II bursts. *Burst rate:* $\sim 20\,\mathrm{h}^{-1}$, then decreasing to $1\,\mathrm{h}^{-1}$. Orbit $\sim 2\,\mathrm{d}$. Source temporarily brightest X-ray source in the sky (several Crab).

Burst oscillations

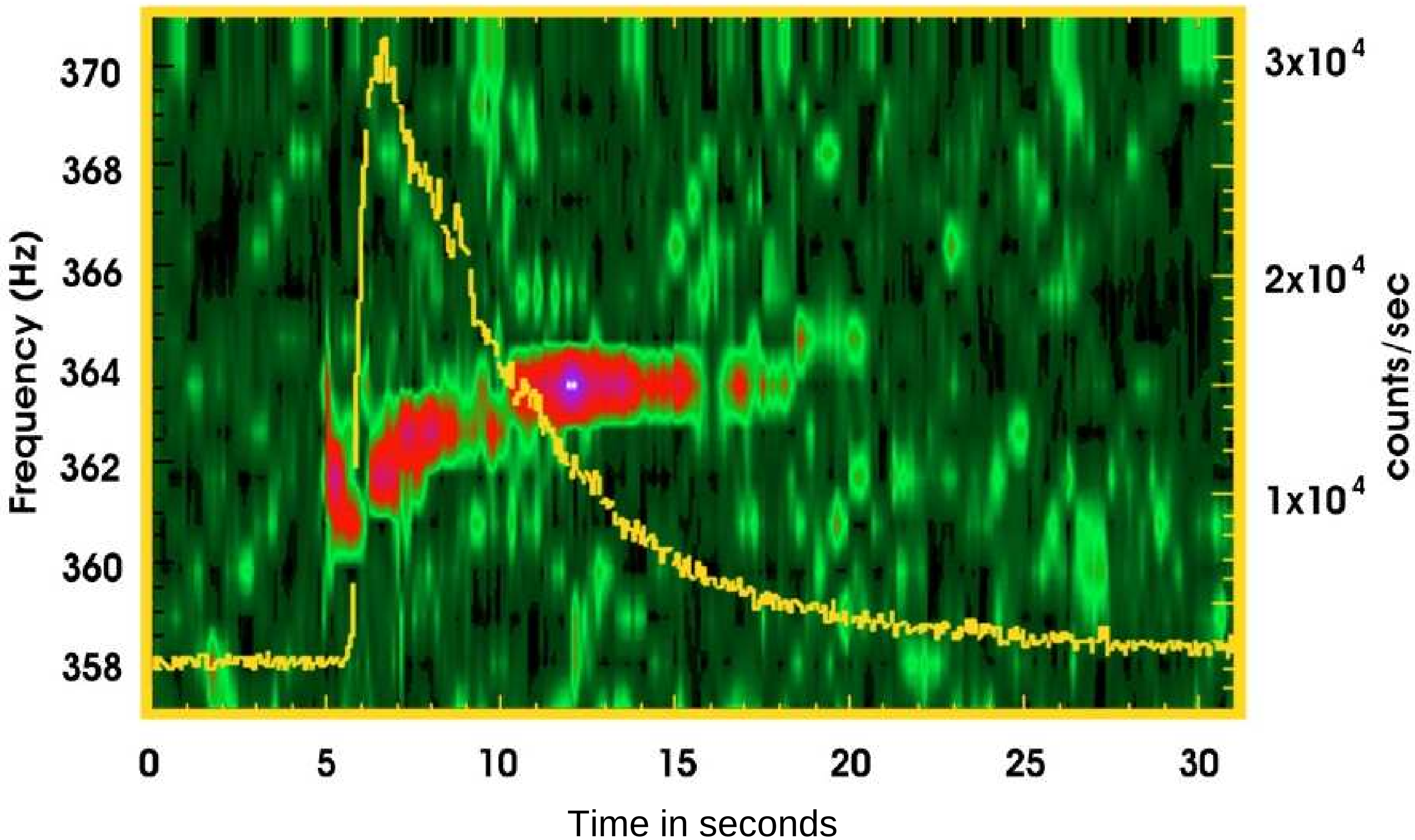

(after Galloway et al., 2006, Fig. 3; colors: power spectrum)

Burst oscillation: strong, coherent oscillation in decay of burst with long term stability. Asymptotic frequency ∼agrees with pulsar rotational frequency

A. Spitkovsky / F. Özel (priv. comm.)

Timing

To describe the variability of an evenly spaced time series $x_k = x(t_k = k\Delta t)$ we use the Discrete Fourier Transform $X_j = X(f_j = j/N\Delta t)$

$$X_j = \sum_{k=0}^{N-1} x_k \exp(2\pi i j k/N) \quad \text{, for } j = 1 \ldots N/2 \tag{6.11}$$

Remember: $\exp(i\phi) = \cos\phi + i\sin\phi$

The amount of variability at a frequency f_j is then characterized by the Power Spectral Density,

$$\mathrm{PSD}_j = A\, X_j^* X_j \tag{6.12}$$

where A is a normalization constant.

To reduce scatter, one often averages the power spectra of several data segments.

The PSD describes the contribution of a given frequency to the total variance of the lightcurve (power).

One often uses the Miyamoto normalization where

$$A_{\text{Miyamoto}} \Longleftrightarrow (\text{rms}/\langle\text{rate}\rangle)^2\,\text{Hz}^{-1} \tag{6.13}$$

EXOSAT: The QPO Era, I

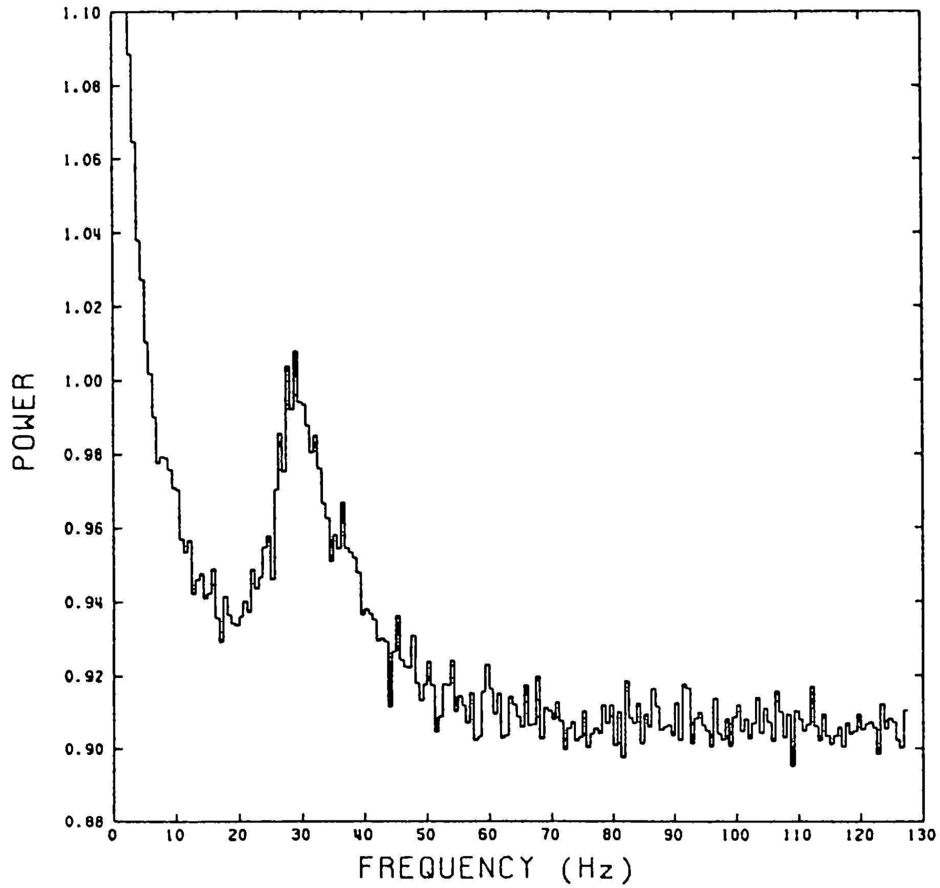

EXOSAT ME: 1–20 keV, $A_{\rm eff} = 1600\,{\rm cm}^2$, $\Delta t \sim 0.25\,{\rm ms}$

1985, IAUC 4043:

"EXOSAT observations of the bright galactic-bulge source GX 5−1 made during 1984 Sept. 18.46−18.83 UT with a time resolution of 0.25 ms show the presence of quasiperiodic oscillations of the 1–10 keV flux with a typical period between 25 and 50 ms [20–40 Hz]."

"Since this is the discovery of a new phenomenon, we urge observers to search for similar X-ray behavior in other sources . . . "

van der Klis, Jansen, van Paradijs, Lewin, van den Heuvel, Trümper, Szatjno

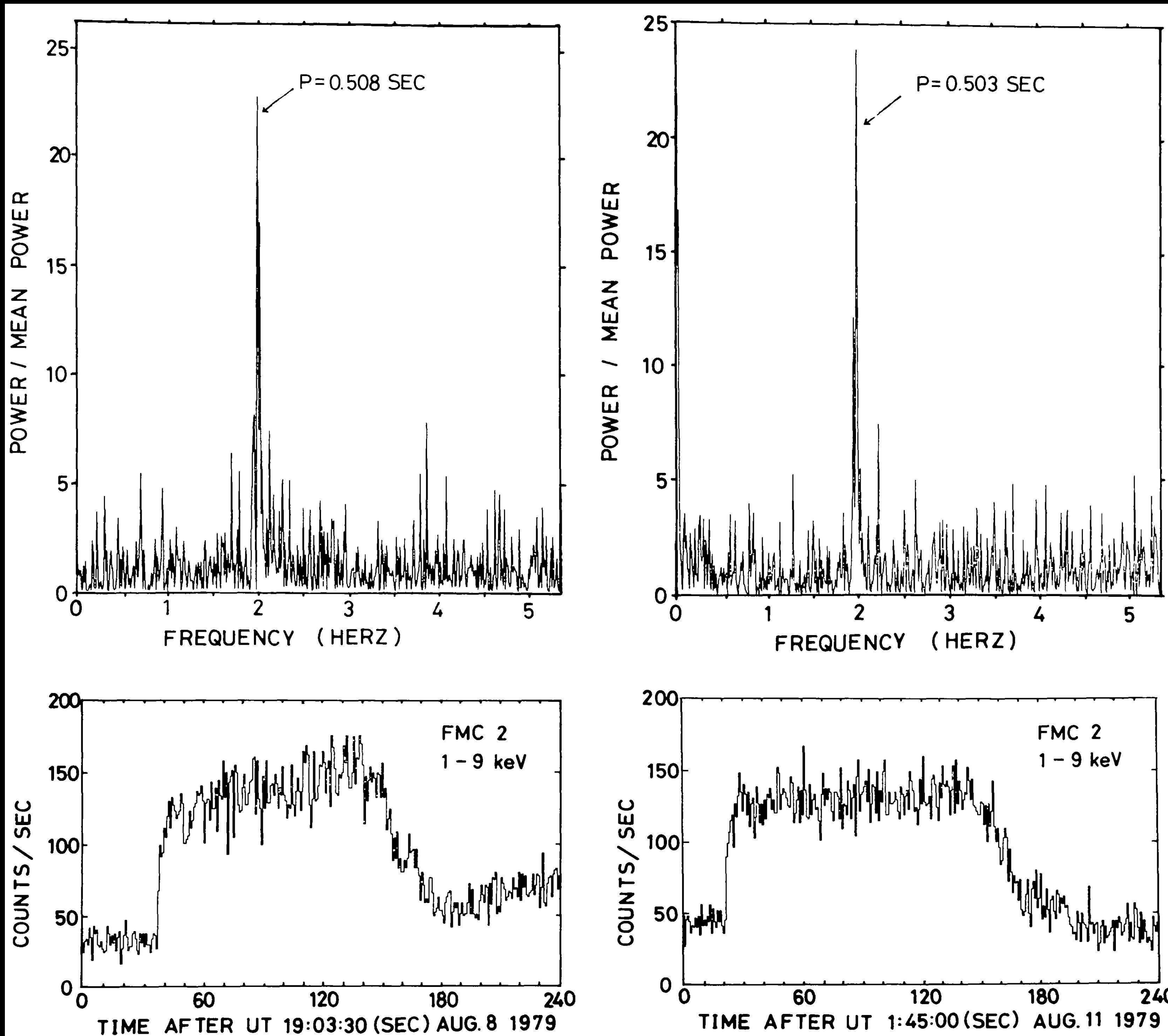

(QPOs during type II bursts of the rapid burster; Lewin, van Paradijs & van der Klis, 1988, Fig. 1.3)

RXTE: The Kilohertz QPO Era, I

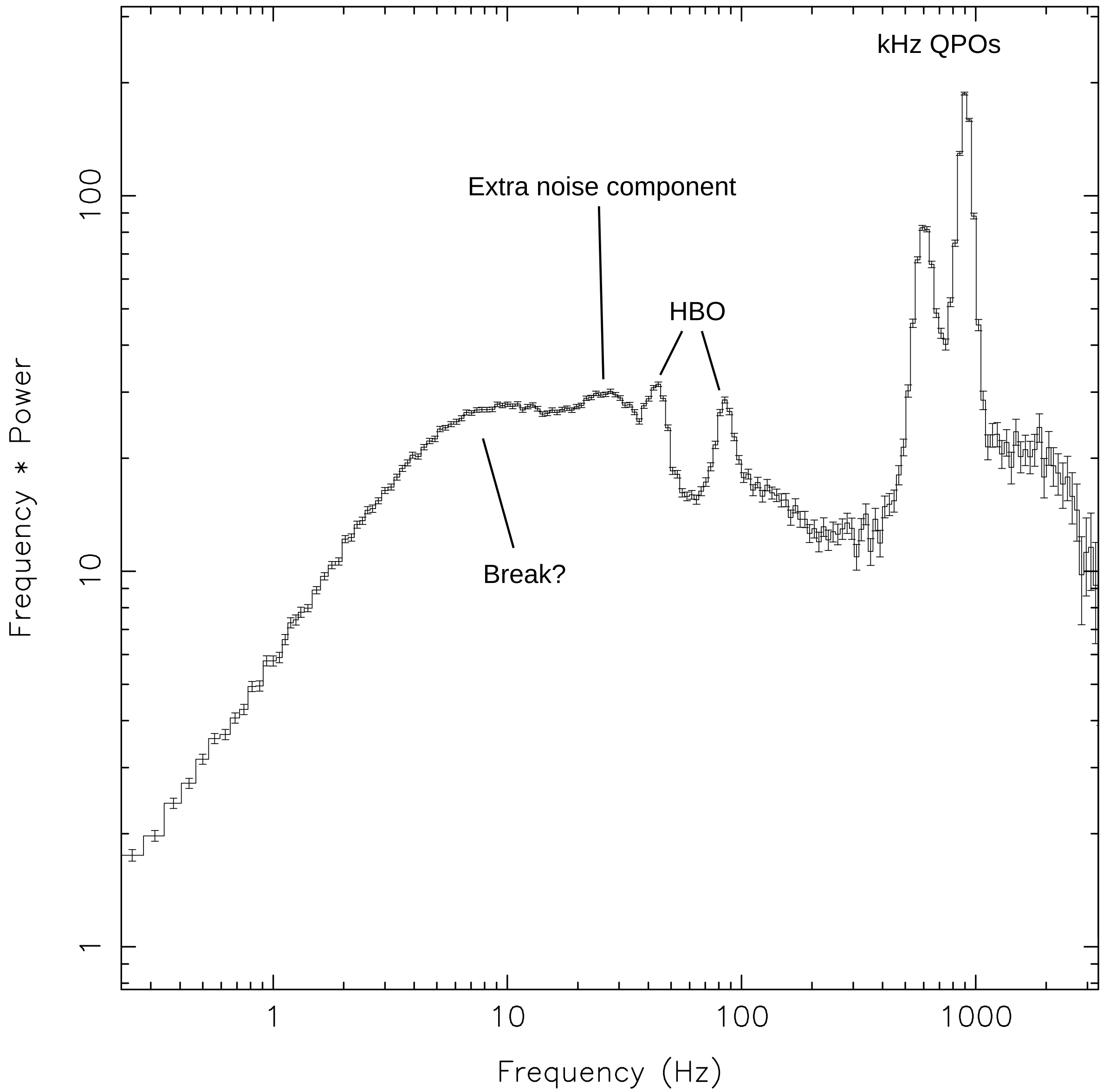

"The kHz QPO are the most important scientific result to date of RXTE".
(http://heasarc.gsfc.nasa.gov/docs/x

RXTE PCA: 2–25 keV, $A_{\text{eff}} = 5000\,\text{cm}^2$, $\Delta t = 1\,\mu\text{s}$

Sco X-1; van der Klis et al., 1996, IAUC 6319, Wijnands & van der Klis (1999)

RXTE: The Kilohertz QPO Era, II

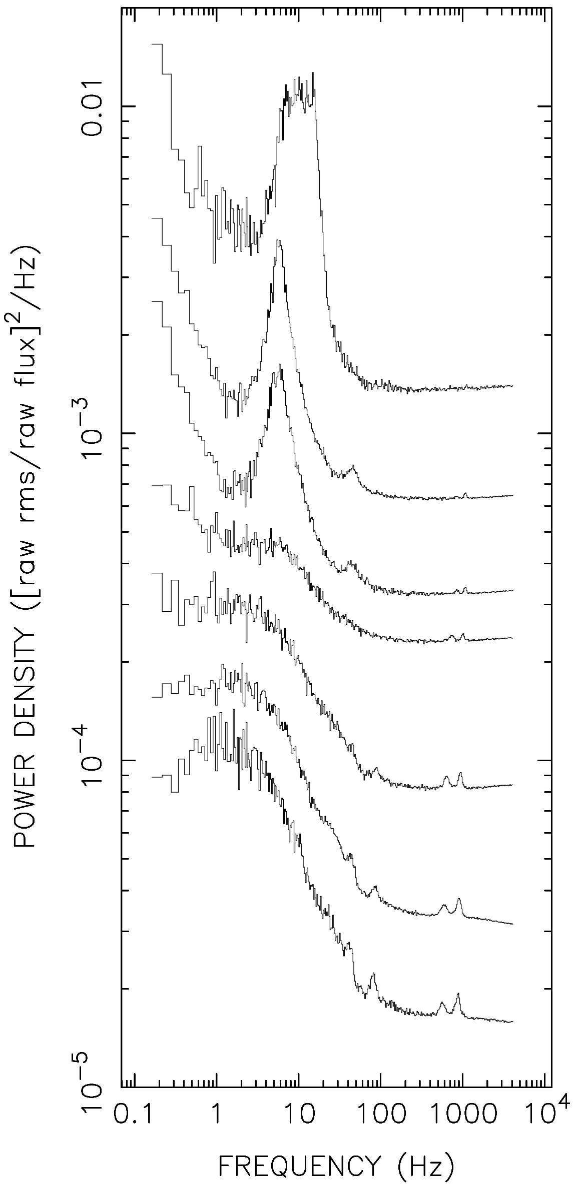

- always have 3 characteristic frequencies:
  - "Low Frequency QPOs" ($\nu_{\rm LF}$): 0.1–100 Hz, many types
  - "kHz Twin Peaks" (ν_1, ν_2): 200–1400 Hz
- "real" kHz QPOs only for neutron star binaries, mostly persistent LMXBs, $\gtrsim$ 20 kHz QPO sources are known, mostly showing double peaks

The kHz QPO strength is flux dependent.

(Wijnands & van der Klis, 1999)

Origin of QPOs

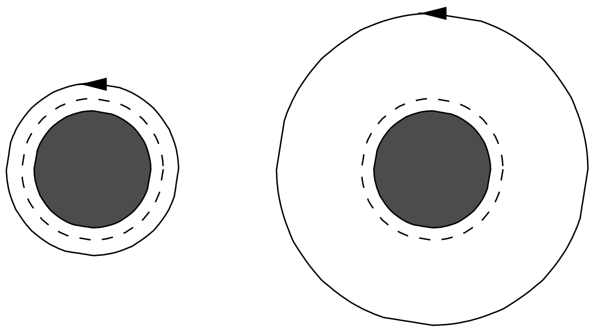

kHZ QPOs occur are on timescales close to the innermost stable circular orbit:

The Keplerian orbit frequency: is

$$\nu_{\text{orb}} = \left(\frac{GM}{4\pi^2 R_{\text{orb}}^3}\right)^{1/2} \approx 1200\,\text{Hz} \left(\frac{R_{\text{orb}}}{15\,\text{km}}\right)^{-3/2} m_{1.4}^{1/2} \qquad (6.14)$$

The edge of the accretion disk is at the innermost stable circular orbit (ISCO), Schwarzschild geometry:

$$R_{\text{ISCO}} = \frac{6GM}{c^2} \sim 12.5 M_{1.4}\,\text{km} \qquad (6.15)$$

and therefore the maximum stable frequency in an accretion disk is

$$\nu_{\text{ISCO}} \sim \frac{1580\,\text{Hz}}{M_{1.4}} \qquad (6.16)$$

Corrections due to the spin of the central object can amount to several 10%

Origin of QPOs

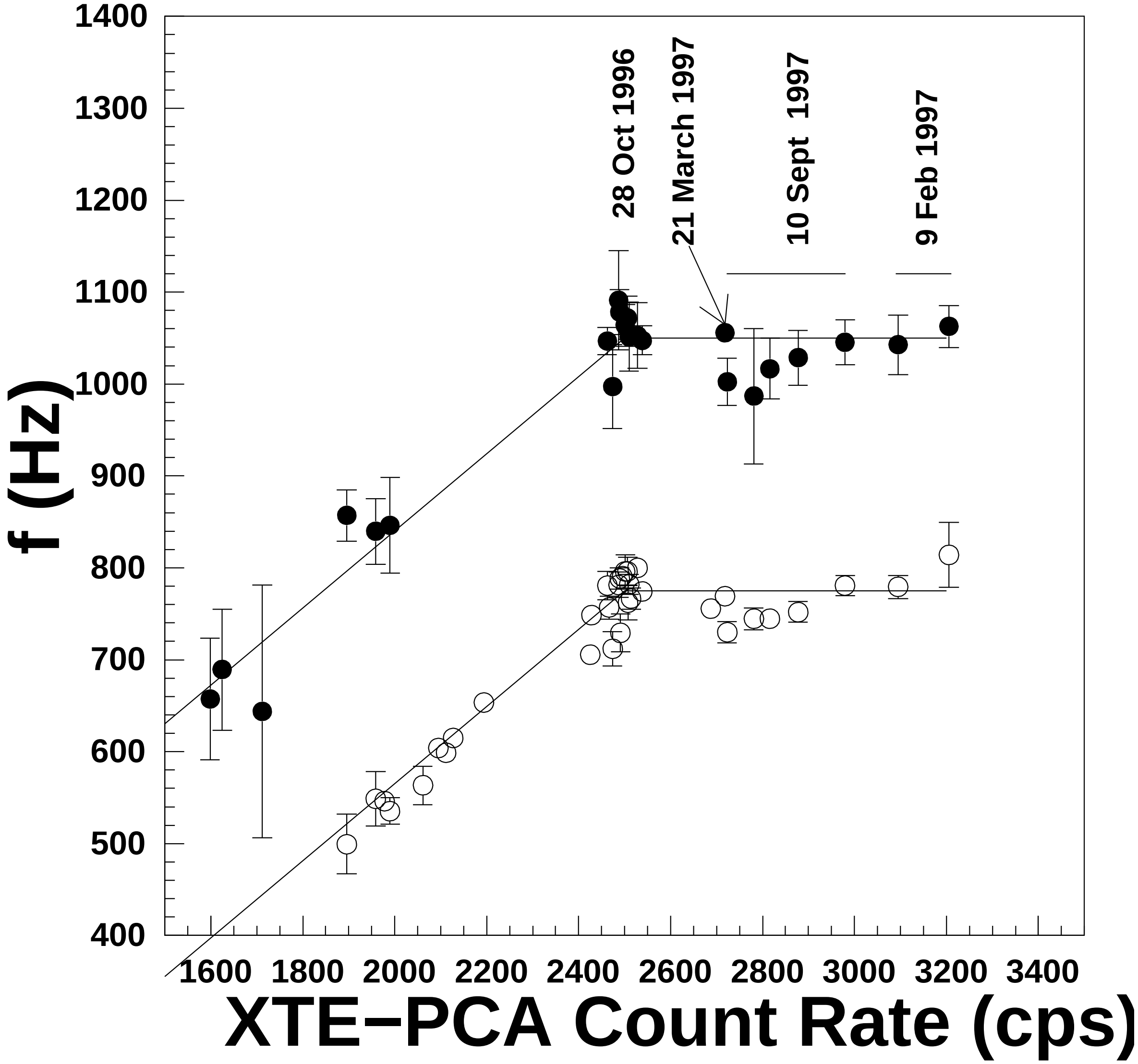

The frequencies of kHz QPOs usually increase with X-ray flux ("parallel-lines phenomenon"), and can saturate at a maximum frequency.

$\Longrightarrow$ Models need to explain ν_{LF}, ν_1, and ν_2.

(4U 1820−30; Zhang et al., 1998)

Beat Frequency Model, I

"beat": resonance between some preferred Keplerian orbit & spin frequency

Magnetospheric BFM:

- preferred radius = Alfvén radius
- orbiting clump ($\nu_{\text{Alfvén}}$) modulated by B-field (ν_{spin})

$\Longrightarrow$ can explain LF QPOs, 5–50 Hz

Sonic Point BFM:

- preferred radius = where radial inflow velocity becomes supersonic, near ISCO
- orbiting clump ($\nu_{\text{sonic}} > \nu_{\text{spin}}$) causes bright footpoint near surface, footpoint: upper kHz QPO, $\nu_2 = \nu_{\text{sonic}}$
- clumps are irradiated with ν_{spin} $\Longrightarrow$ footpoint emission is modulated with beat between ν_{sonic} and ν_{spin}, footpoint modulation: lower kHz QPO, $\nu_1 = \nu_{\text{beat}}$

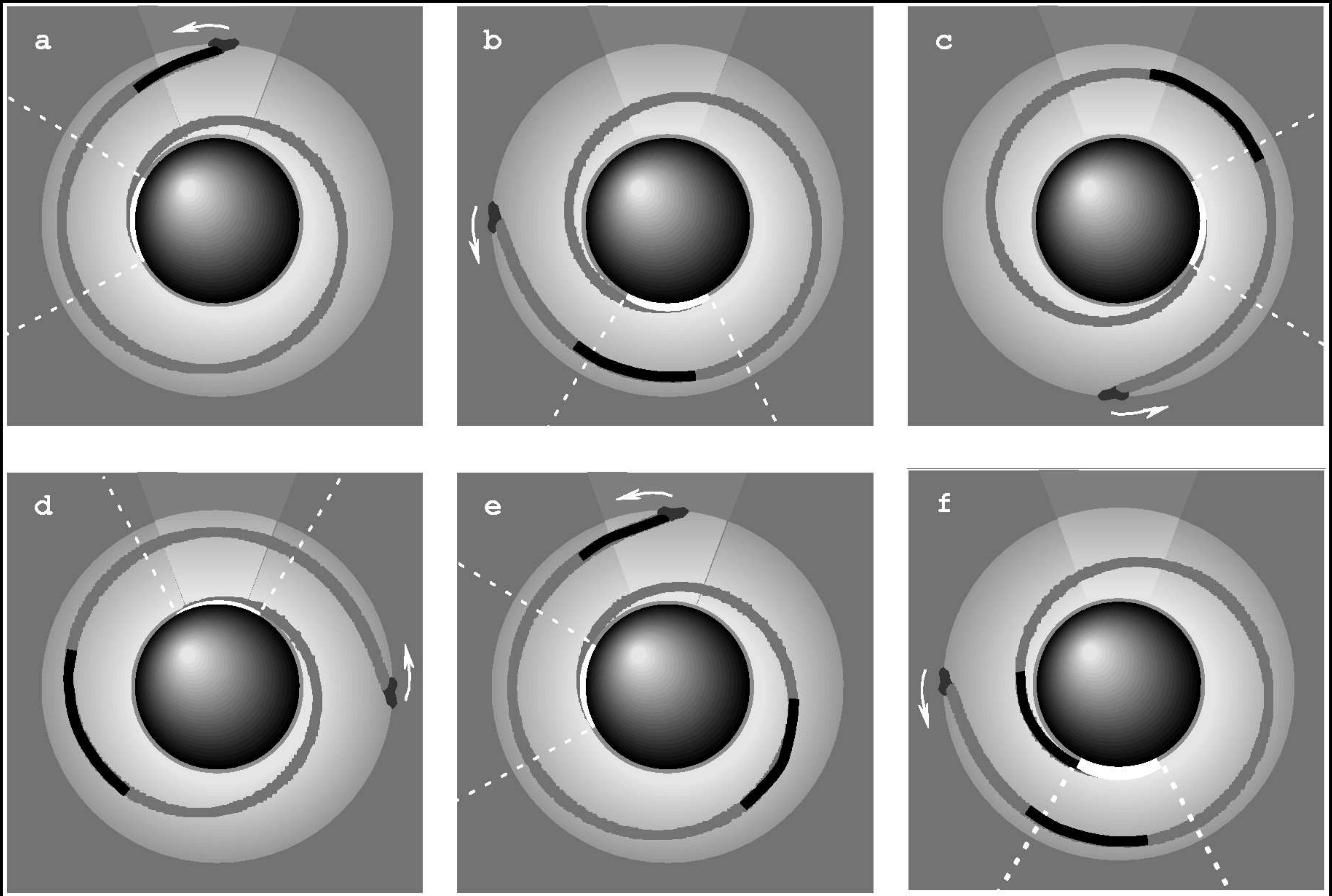

(Miller, Lamb & Psaltis, 1998)

Beat Frequency Model, III

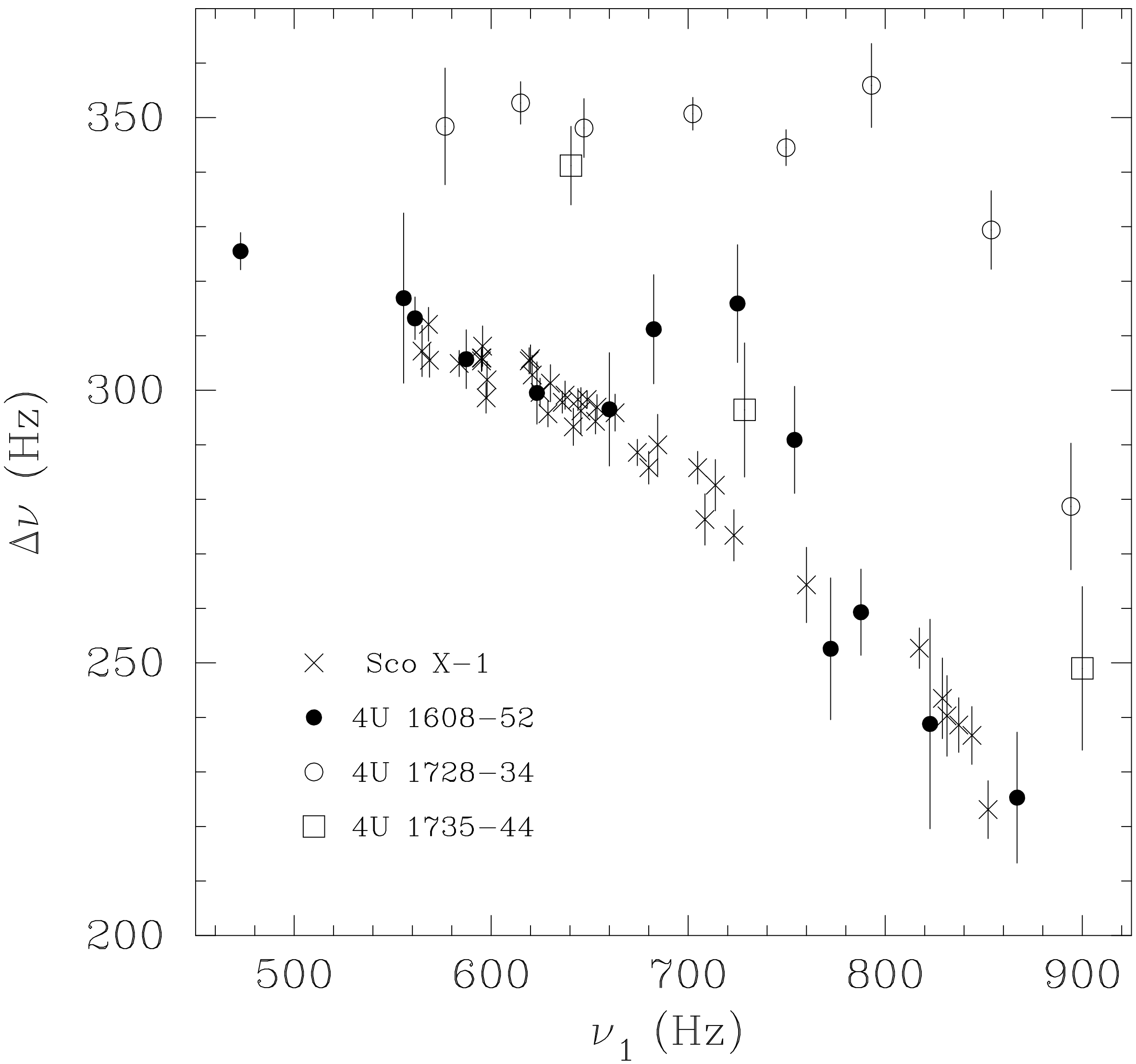

There is a varying frequency separation between the kHz QPOs of different sources

$\Longrightarrow$ problem for the beat frequency model?

(van der Klis, 2000)

Beat Frequency Model, IV

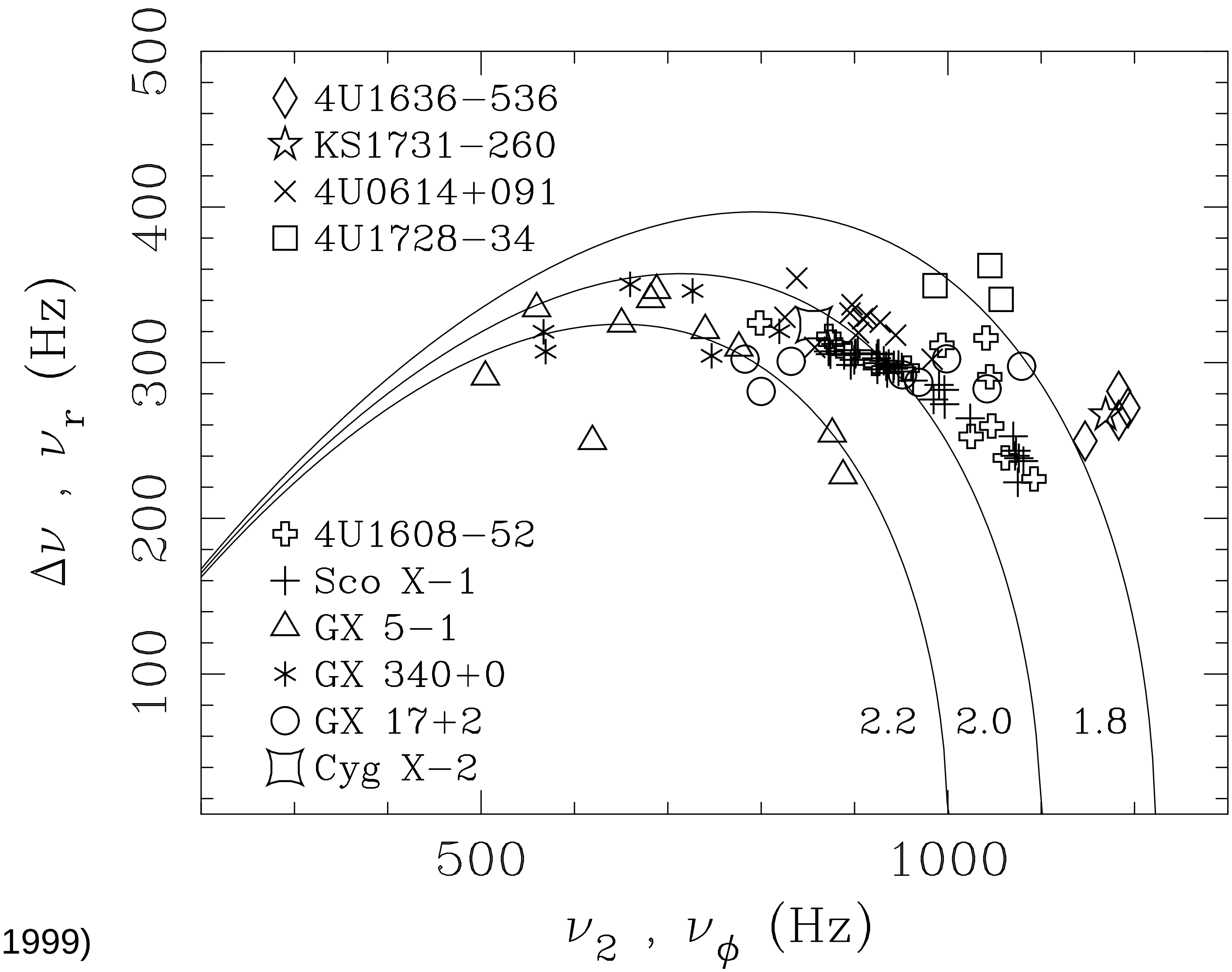

(Stella & Vietri, 1999)

The frequency separation of the QPOs varies differently in different sources.

Beat Frequency Model, V

Properties & problems of the sonic point beat frequency model:

- needs surface
  $\Longrightarrow$ not valid for BHC sources
- Keplerian motion inside $r_{\text{Alfén}}$
- r_{sonic} depends on $\dot{M}$
  $\Longrightarrow$ varying ν_2 can be explained
- $\Delta\nu = \nu_2 - \nu_1$, constant, can be $< \nu_{\text{spin}}$
  $\Longrightarrow$ varying $\Delta\nu$ cannot easily be explained
- predicts additional frequencies (differing from precession model)

Relativistic Precession Model, I

General Relativity: free-particle orbits show characteristic frequencies

Idea of the model:

- disk is disrupted near ISCO, forming blobs
- blob orbits are inclined and eccentric

Characteristic frequencies:

- orbit frequency: upper kHz QPO, ν_2
- periastron precession: lower kHz QPO, ν_1
- relativistic frame dragging $\longrightarrow$ "wobble of the orbital plane":

  nodal precession (Lense-Thirring)

  $\nu_{\mathrm{LF}} = 2 \times \nu_{\mathrm{nod}}$

  $\nu_{\mathrm{nod}} = 8\pi^2 I\, \nu_2^2 \nu_{\mathrm{spin}} / c^2 M$, where I: moment of inertia

see, e.g., Stella & Vietri (1998)

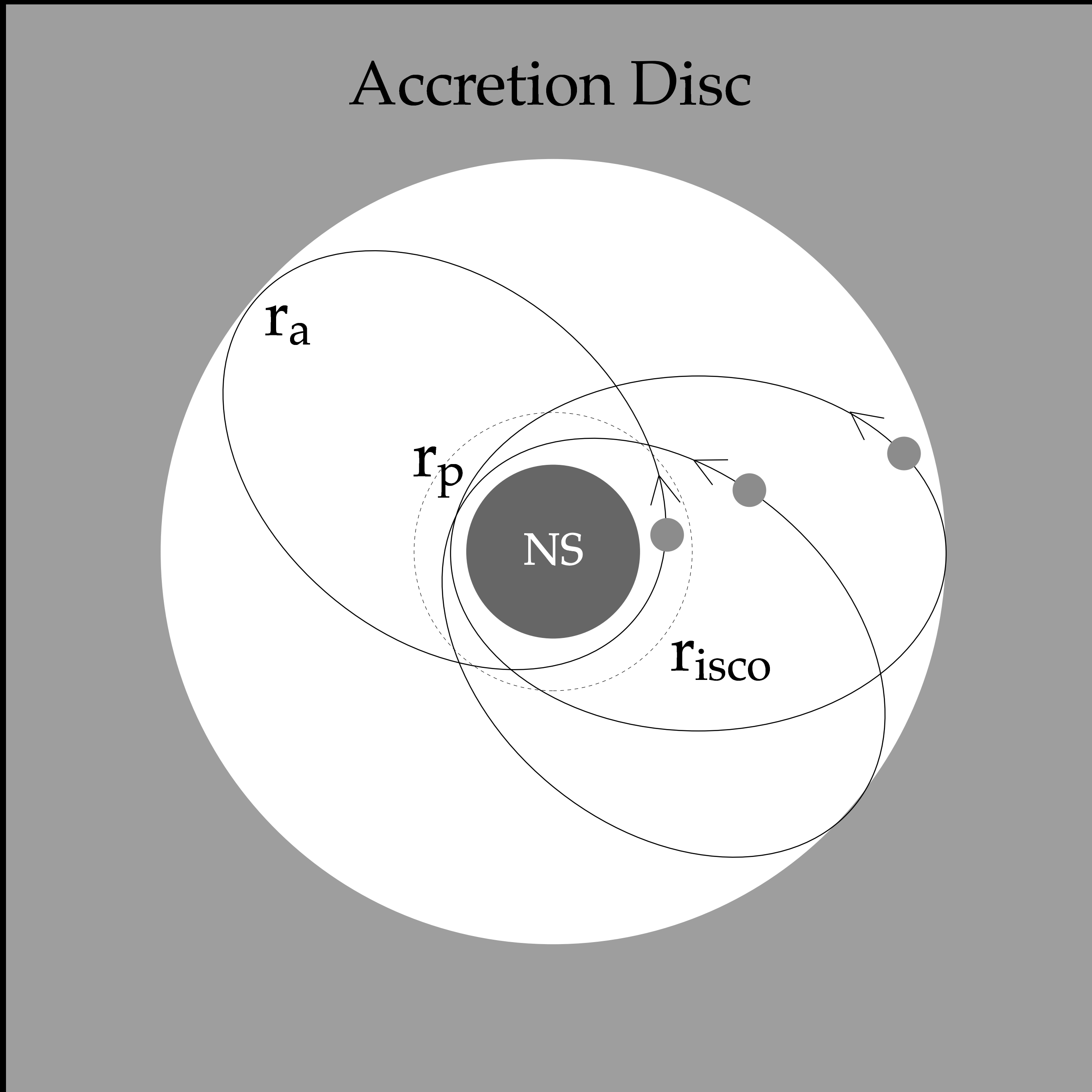

(Marković & Lamb, 1998, see also Marković & Lamb, 2000, astro-ph/0009169)

Relativistic Precession Model, III

Properties & problems of the RPM:

- does not need surface
  $\Longrightarrow$ also valid for BHC sources
- can explain $\Delta\nu$ (more or less)
- how to disrupt the disk?
  how to create compact clumps?
  how to maintain tilted orbits?
- how to create the flux modulations?
- other frequencies could be more important

Model Summary

Promises:

- constrain M and R (via kHz QPOs)
  $\Longrightarrow$ constrain Equation of State for neutron stars
- constrain spin
  ("holy grail", LMXB/ms radio pulsar evolution?!)
- constrain B-field (via LF QPOs)
- observe GR effects

Difficulties:

- observations (varying $\Delta\nu_{\text{kHz}}$, ν-correlations)
  triggered evolution of many different models (>12)
- no individual model does address all issues
  (i.e, generation of flux modulation, …)
- models predict different ν_{spin} and M, e.g.,
  BFM: $\nu_{\text{spin}} = 250$–350 Hz
  RPM: $\nu_{\text{spin}} = 300$–900 Hz
- what about "surface models"? $\Longleftrightarrow$ big question: do BHCs show the same behavior as neutron star XRBs?

Church, M. J., 2004, in Revista Mexicana de Astronomia y Astrofi sica Conference Series, ed. G. Tovmassian, E. Sion, Vol. 20, 140

Church, M. J., & Balucinska-Church, M., 1995, A&A, 300, 441

Cumming, A., 2004, Nucl. Phys. B Proc. Suppl., 132, 435

Cumming, A., & Bildsten, L., 2001, ApJ, 559, L127

Galloway, D. K., Muno, M. P., Hartman, J. M., Savov, P., Psaltis, D., & Chakrabarty, D., 2006, ApJS, submitted (astro-ph/0608259)

Grimm, H.-J., Gilfanov, M., & Sunyaev, R., 2003, Ch. J. Astron. Astrophys. Suppl., 3, 257

Hansen, C. J., & van Horn, H. M., 1975, ApJ, 195, 735

Hasinger, G., & van der Klis, M., 1989, A&A, 225, 79

Jonker, P. G., et al., 2000, ApJ, 537, 374

Joss, P. C., & Rappaport, S. A., 1984, Ann. Rev. Astron. Astrophys., 22, 537

Kuulkers, E., 2004, Nucl. Phys. B Proc. Suppl., 132, 466

Lamb, D. Q., & Lamb, F. K., 1978, ApJ, 220, 291

Lewin, W. H. G., van Paradijs, J., & Taam, R. E., 1993, Space Sci. Rev., 62, 223

Lewin, W. H. G., van Paradijs, J., & van der Klis, M., 1988, Space Sci. Rev., 46, 273

Marković , D., & Lamb, F. K., 1998, ApJ, 507, 316

Méndez, M., van der Klis, M., Ford, E. C., Wijnands, R., & van Paradijs, J., 1999, ApJ, 511, L49

Miller, M. C., Lamb, F. K., & Psaltis, D., 1998, ApJ, 508, 791

Mitsuda, K., Inoue, H., Nakamura, N., & Tanaka, Y., 1989, PASJ, 41, 97

Schatz, H., & Rehm, K. E., 2006, Nucl. Phys. A, 777, 601

Stella, L., & Vietri, M., 1998, ApJ, 492, L49

Stella, L., & Vietri, M., 1999, Phys. Rev. Lett., 82, 17

Strohmayer, T., & Bildsten, L., 2006, in Compact stellar X-ray sources, ed. W. Lewin, M. van der Klis, (Cambridge: Cambridge Univ. Press), 113–156

Swank, J. H., Becker, R. H., Boldt, E. A., Holt, S. S., Pravdo, S. H., & Serlemitsos, P. J., 1977, ApJ, 212, L73

Taam, R. E., & Picklum, R. E., 1979, ApJ, 233, 327

van der Klis, M., 1989, Ann. Rev. Astron. Astrophys., 27, 517

van der Klis, M., 2000, Ann. Rev. Astron. Astrophys., 38, 717

van Straaten, S., van der Klis, M., & Méndez, M., 2003, ApJ, 596, 1155

White, N. E., Stella, L., & Parmar, A. N., 1988, ApJ, 324, 363

Wijnands, R., & van der Klis, M., 1999, ApJ, 514, 939

Zhang, W., Smale, A. P., Strohmayer, T. E., & Swank, J. H., 1998, ApJ, 500, L171

Zingale, M., et al., 2001, ApJS, 133, 195

Black Hole Binaries